Identification of Chemical Constituents on Anti-osteoclastogenesis Activity of Dragon's Blood (Daemonorops Draco)

Identification of Chemical Constituents on Anti-osteoclastogenesis Activity of Dragon's Blood (*Daemonorops Draco*)

[抗破骨細胞形成に及ぼす龍血(*Daemonorops Draco*)中の活性成分の同定]

2019

The United Graduate School of Agricultural Science, Gifu University

Science of Biological Resources

(Gifu University)

WANG XIAOYU

Identification of Chemical Constituents on Anti-osteoclastogenesis Activity of Dragon's Blood (*Daemonorops Draco*)

[抗破骨細胞形成に及ぼす龍血(*Daemonorops Draco*)中の活性成分の同定]

WANG XIAOYU

CONTENTS

List of figures

List of tables

Dedication

It is with my deepest and warmest affection.

This thesis is dedicated to my beloved and sweet parents, for their unconditional love, encouragement and support throughout my entire study. Without them, none of this would have happened.

Also, this thesis is dedicated to my gracious and respectable supervisor, Prof. Mitsunaga Tohru, a friend and mentor who spent his countless hours of reflecting, reading, encouraging and most of all patience to help my continuous self-improvement.

In the end, I dedicate this thesis to all my lab members who helped me a lot during my research time, and to all those who have faith in the power of science.

Acknowledgement

This dissertation is a part of fulfillment of the requirement for the degree of PhD under the supervision of Prof. Mitsunaga Tohru, the United Graduate School of Agricultural Science, Gifu University, Japan.

This thesis includes all of the results of my experiments which were performed since 2016 until 2019.

With boundless love and appreciation, I would like to extend my heartfelt gratitude and appreciation to people who helped me bring this study into reality. I would like to extend my profound gratitude to the following:

We greatly appreciate Professor Irmanida Batubara and acknowledge the D.I.A for support of preparing tested sample *Daemonorops Draco*.

My supervisor, Prof. Mistunaga Tohru whose expertise, consistent guidance, ample time spent and consistent advices that helped me make this study accomplished. I acknowledge my sincerest appreciation for his great support, patience and suggestions during my entire research.

My dear and beloved parents, who have supported to me all the time without asking anything for return, are my motivation for the past two three years. I am extremely grateful for their maximum understanding; moral and financial supporting and selfless love which helped me finish my master study.

I would love to especially thank Mr. Yuya Kakumu, who has done the methanol extract part and brought it from Indonesia. And also all members in my lab, for their great kindness and helping me use all the facilities to complete my PhD study.

Summary

Metabolic bone diseases are characterized by defects in the processes of bone resorption, formation and mineralization, include osteoporosis, rheumatoid arthritis, rickets (children) / osteomalacia (adults), Paget's disease, etc. Osteoporosis is the most common reason for a broken bone among the elder people worldwide, caused by the imbalance level of bone resorption and bone formation. Bone resorption is associated with excessive formation of osteoclast, so called "osteoclastogenesis", and acid phosphatase activity.

To date, the main anti-bone resorption drugs used for patients are bisphosphonates and denosumab, and they may give severe side effects in long-term treatment, such as gastrointestinal adverse, to cause worse health problems. Natural products have been studies over 100 years for not pharmaceutical products and drugs. Especially, folk medicine has an advantage over other natural products because of its long-and safe-use history.

For these reasons, we attempted to evaluate the anti-osteoclastogenesis activity using 10 medicinal plant crude extracts, which might provide new effective drugs or clinical candidates for treatment of metabolic bone disease. This research is divided into three chapters including general introduction, natural compounds isolated from *Daemonorops draco*, anti-osteoclastogenesis activity evaluation of isolated compounds & 19 commercial flavonoids and elucidation on structure-activity relationship (SAR).

Chemical constituents from *D.draco* and anti-osteoclastogenesis activity

Chapter 2, among 10 species medicinal plants extracts including *Murraya paniculata* **(S1)**, *Guazuma ulmifolia* **(S2)**, *Orthosiphon aristatus* **(S3)**, *Sinapis arvensis* **(S4)**, *Syzyguim polyanthum* **(S5)**, *Andrographis paniculata* **(S6)**, *Zingiber purpureum* **(S**7), *Kaempferia galangal* **(S8)**, *Zingiber officinale* **(S9)**, *Daemonorops draco* **(S10)** were examined for anti-osteoclastogenesis activity. Among them, *D. draco* **(S10)** extract had shown as the most effective one on anti-osteoclastogenesis activity. *Daemonorops* is a genus of rattan palms in the Arecaceae family found primarily in the tropics and subtropics in Southeast Asia with a few species extending into southern China and the Himalayas. It has been used as traditional medicines since lone time ago due to its antiviral, antibacterial and antifungal properties.

The MeOH extracts was repeatedly chromatographed on silica gel, Sephadex LH-20 and ODS-3 columns to obtain 6 compounds: 4 flavonoid (**1, 2, 4, 6**) and 2 benzoic acids (**3, 5**). The structures of these compounds were elucidated by nuclear magnetic resonance (NMR) experiments and confirmed by comparing with previous reports. The anti-osteoclastogenesis activity of the isolated compounds was furtherly investigated by osteoclastogenesis assay. Moreover, 19 commercial flavonoids were used for the evaluation of anti-osteoclastogenesis activity also to establish their SAR profile.

As shown in Figure 2.8, com.**1** was identified as a novel flavan compound and exhibited the most potent inhibition on osteoclastogenesis, inhibited 78%

osteoclastogenesis activity at 10μM without any cytotoxicity and completed inhibition of osteoclastogenesis activity at 100μM with 75% cell viability. Com.**2** showed 50% inhibition on osteoclastogenesis activity, with no cytotoxicity at 10μM. Moreover, combined with comparison of the structure by com.**1** and com.**2** indicated that the presence of 7-methoxy in flavan structure was crucial for anti-osteoclastogenesis activity. Com.**3** and com.**5** displayed 75% and no inhibition on osteoclastogenesis activity at 100μM respectively. Com.**4**, identified as novel componud, and com.**6** showed slight inhibition, with 27% and 35% anti-osteoclastogenesis activity respectively.

Elucidation on structure-activity relationship

To furtherly elucidate more information of SAR in flavonoid skeleton, nineteen commercial flavonoids: baicalein, luteolin, kaempferol, quercetin, myricetin, apigenin, galangin, chrysin, taxifolin, 3-hydroxyflavone, 7- hydroxyflavone, robinetin, (-)-epicatechin, (-)-catechin, flavone, flavanone, morin, naringenin and hesperetin, were performed on anti-osteoclastogenesis activity at 10μM.

Baicalein exhibited the excellent anti-osteoclastogenesis activity with completed inhibition, was the most effective compound among 19 flavonoids and isolated compounds. Galangin showed similar inhibitory activity (73% inhibition) as com.**1** (78% inhibition). As well, quercetin, chrysin, 3-hydroxyflabone, 7-hydroxyflavone and flavanone exhibited 66%, 52%, 59%, 55% and 62% inhibition respectively.

Comparison on anti-osteoclastogenesis of baicalein, luteolin and quercetin indicated that the absence of hydroxyl groups on B-ring is essential for anti-osteoclastogenesis activity. Moreover, comparison of anti-osteoclastogenesis between 3-hydroxyflavone, 7-hydroxyflavone, and flavone indicated that neither 7-hydroxyl group nor 3-hydroxyl group provide anti-osteoclastogenesis activity in flavone skeleton. Interestingly, (3R)-hydroxyl group seems to provide much more effective activity on osteoclastogenesis inhibition than (3S)-hydroxyl group by comparing with (-)-epicatechin and (-)-catechin. Also, double bond at C-2 and C-3 position increase anti-osteoclastogenesis activity by comparing apigenin and naringenin.

All these information were used to establish the first SAR profile in flavonoid skeleton on anti-osteoclstogenesis activity.

学位論文要旨

代謝性骨疾患は、骨吸収、形成および石灰化の過程における欠陥を特徴とし、骨粗鬆症、関節リウマチ、くる病(小児)/骨軟化症(成人)、ページェット病などを含む。骨粗鬆症は、骨吸収と骨形成の不均衡レベルによって引き起こされる、これは世界中の高齢者における骨折の最も一般的な理由である。骨吸収は、破骨細胞の過剰な形成、いわゆる「破骨細胞形成」および酸性ホスファターゼ(TRAP)活性と関連している。

現在までのところ、患者に使用される主な骨吸収抑制薬はビスフォスフォネート剤およびデノスマブであり、これらは長期治療において胃腸への副作用が問題となっている。一方、天然物由来の薬剤は、100 年以上にわたって医薬品や医薬部外品への利用研究が行われてきており、骨粗鬆症治療薬においても副作用の少ない天然医薬品の開発が望まれている。

著者らは、代謝性骨疾患治療のための新しい有効な天然薬剤または臨床的にも応用可能な候補として 10 種の薬用植物粗抽出物を用いて、抗破骨細胞形成活性を評価することを試みた。本研究は、第 1 章で序論、第 2 章で *Daemonorops draco* から単離された化合物の同定、第 3 章では、単離された化合物および 19 種の市販フラボノイドの抗破骨細胞活性評価、および構造活性相関(SAR)の解明からなる。

D.draco 由来の化学成分と抗破骨細胞形成活性

第 2 章では、*Murraya paniculata* (S1)、*Guazuma ulmifolia* (S2)、*Orthosiphon aristatus* (S3)、*Sinapis arvensis* (S4)、*Syzyguim polyanthum* (S5)、*Andrographis*

paniculata (S6)、*Zingiber purpureum* (S7)、*Kaempferia galangal* (S8)、*Zingiber officinale* (S9)、*Daemonorops draco* (S10)の 10 種の薬用植物抽出物の抗破骨細胞形成活性について調べた。その中で *D. draco* (S10)抽出物は抗破骨細胞形成活性に最も有効であることが示された。*D. draco* は、主に東南アジアの熱帯および亜熱帯で見られる Arecaceae 科のガラガラ属の一種で、数種が南シナおよびヒマラヤにも分布している。古くから抗ウイルス、抗菌、抗真菌の性質から伝統的医薬品として用いられてきた。

MeOH 抽出物は、シリカゲル、Sephadex LH-20 および ODS-3 カラムを繰り返し行い、6 つの化合物、4 種のフラボノイド(**1, 2, 4, 6**)および 2 種の安息香酸(**3**、**5**)を得た。これらの化合物の構造を核磁気共鳴(NMR)実験により解明し、以前の報告と比較して同定した。単離した化合物の抗破骨細胞形成活性を、破骨細胞形成アッセイによりさらに調べた。さらに、19 種の市販フラボノイドを抗破骨細胞形成活性の評価に使用し、それらの SAR プロファイルを確立した。

化合物 **1** は新規フラバン化合物として構造決定され、破骨細胞形成に対して最も強力な阻害を示し、細胞毒性を示さない 10 μM の添加で 78%の破骨細胞活性阻害率を示し、75%の細胞生存率を示す 100 μM では、破骨細胞活性を完全に阻害した。化合物 **2** は、破骨細胞活性を 50%阻害し、10 μM では細胞毒性を示さなかった。さらに、化合物 **1** および化合物 **2** による構造の比較から、フラバン構造中の 7 位メトキシル基の存在が抗破骨細胞活性に重要であることが示された。化合物 **3** は 100 μM の濃度で 75%の破骨細胞形性阻害で、化合物 **5** は同濃度でまったく活性を示さなかった。新規成分として同定された化合物 **4** および化合物 **6** は、それぞれ 27%および

35%の抗破骨細胞活性でありわずかな阻害を示した。

構造活性相関の解明

フラボノイド骨格におけるSARのさらなる情報を解明するために、19種の市販フラボノイド:バイカレイン、ルテオリン、ケンフェロール、ケルセチン、ミリセチン、アピゲニン、ガランギン、

クリシン、タキシホリン、3-ヒドロキシフラボン、7-ヒドロキシフラボン、ロビネチン、(-)-エピカテキン、(-)-カテキン、フラボン、フラバノン、モリン、ナリンゲニン、およびヘスペレチンを、10 μ M で抗破骨細胞形成活性を実施した。

バイカレインは優れた抗破骨細胞形成活性を示し、ほぼ完全に阻害し、19 のフラボノイドおよび単離化合物の中で最も有効な化合物であった。ガランギンは化合物1(78%阻害)と同様の阻害活性(73%阻害)を示した。同様に、クエルセチン、クリシン、3-ヒドロキシフラボーン、7-ヒドロキシフラボンおよびフラバノンは、それぞれ 66%、52%、59%、55%および 62%の阻害率であった。

バイカレイン、ルテオリンおよびケルセチンの比較から、B 環上のヒドロキシル基の欠如が抗破骨細胞形成活性に必須であることを示した。さらに、3-ヒドロキシフラボン、7-ヒドロキシフラボン、およびフラボンの抗破骨細胞形成の比較から、7-ヒドロキシル基および 3-ヒドロキシル基は抗破骨細胞形成活性に影響しないことを示した。興味深いことに、(-)-エピカテキンと(+)-カテキンの比較から、(3R)-ヒドロキシル基は、(3S)-ヒドロキシル基よりも破骨細胞形成阻害に対してはるかに有効な活性を示した。また、アピゲニンとナリンゲニンの比較から、C-2 と C-3 位の二重結合は、抗破骨細

胞形成活性を増強することが明らかとなった。

これらの情報は、フラボノイド骨格における抗骨形成活性に関するはじめての SAR プロファイルの確立として有用である。

Chapter 1

General Introduction

1.1 Metabolic bone disease

Metabolic bone diseases are characterized by defects in the processes of bone resorption, formation and mineralization (Bischi et al., 2010). The term ‘metabolic bone disease’ has been used since 1948, when Albright and Reifenstein used it to explain conditions that influenced on the processes of bone formation and remodeling involving the whole skeleton (Albright et al., 1948). Metabolic bone disease is the third most common endocrine disorder following diabetes and thyroid diseases. Examples of metabolic bone diseases include osteoporosis, rickets (children) / osteomalacia (adults) Paget’s disease, tumor induced osteomalacia, fibrous dysplasia, osteogenesis imperfecta and so on (Bhansali, 2012).

1.1.1 Osteoporosis

Osteoporosis is a systemic skeletal disease, a growing public health disease worldwide, characterized by low bone density and microarchitectural deterioration of bone tissue, with a consequent increase in bone fragility (Yokoyama et al., 2012 and Tan et al., 2014). It is caused by the imbalance between bone resorption and bone formation (Wu et al., 2009). Bone resorption is associated with excessive formation of osteoclast and acid phosphatase activity; whereas bone formation is related to osteoblast proliferation, alkaline phosphatase activity, mineralization and collagen production (Manolagas, 2000).

Osteoporosis is the most common reason for a broken bone among the elder

people (https://www.niams.nih.gov/health-topics/osteoporosis). Bones that normally break include the spine, the forearm, and the hip (Notelovitz, 1993). Normally there are no symptoms until a broken bone typically occurs. However, decreased ability to carry out normal activities may happen due to chronic pain after a broken bone. Bones may be fragile to such a degree that a break may occur by minor stress or spontaneously (https://www.niams.nih.gov/health-topics/osteoporosis).

To date, bisphosphonates (alendronate, ibandronate, risedronate and zoledronate) (Figure 1) are currently the most important class of anti-osteoclastogenesis agents used in the treatment of metabolic bone diseases (Rogers et al., 2000); however, oral administration of bisphosphonates is associated with significant side effects, such as gastrointestinal adverse (Conte et al., 2004).

Osteoporosis is also an age-related bone disorders owning to the close relationship between the aging process of bone and the pathogenesis of osteoporosis, resulting in bone loss and micro-architecture, with increasing risk to fragility fractures (Raisz et al., 2003). With increasing age, bone remodeling is degenerated leading to bone imbalance at individual bone metabolic unit sites. And after the fourth decade of life, there is a decrease in the formation of periosteal bone, on the contrast, increasing number of remodeling units within endosteal bone occurs at the same time in both men and women (Kawai et al., 2012).

1.1.2 Rheumatoid arthritis

Rheumatoid arthritis is a long-term autoimmune disorder, characterized by synovial inflammation and hyperplasia (“swelling”), autoantibody production and bone destruction (“deformity”) (McInnes et al., 2011).

The bone destruction in rheumatoid arthritis patients is observed in joints, typically resulted in warm, swollen and joint pain. Osteoclasts are known to play a crucial role in the pathogenesis of bone destruction in rheumatoid arthritis. Also, excessive levels of osteoclast formation in synovial cell cultures were obtained from patients with rheumatoid arthritis. Thus, bone destruction in rheumatoid arthritis mainly due to the abnormal differentiation and activation of osteoclasts, which is called osteoclasogenesis (Sato et al., 2006).

1.1.3 Paget’s disease

Paget's disease is a condition involving cellular remodeling and deformity of one or more bones. Other than osteoporosis and rheumatoid arthritis occur in entire skeleton, Paget’s disease one or multiple bones of the body (mostly in pelvis, femur, lumbar vertebrae, and skull (Paul Tuck et al., 2017 and Ralston et al., 2012). The affected bones observed under microscope show dysregulated bone remodeling, such as excessive bone breakdown and subsequent disorganized new bone formation. These skeleton disorders lead to weak bone, furtherly resulting in deformity, pain, fracture, or arthritis of associated joints (Paul Tuck et al., 2017).

Paget’s disease progress is basically described as followed:

Primarily, the increase of local bone resorption is caused by large and numerous osteoclasts and furtherly developed into an advancing lytic wedge in long bones or the skull, which is called osteoporosis. Then, osteolysis may occur due to compensatory increase of bone formation induced by locally recruited osteoblasts, which is associated with accelerated deposition of lamellar bone and resulted in a chaotic bone net of trabecular bone rather than the normal linear lamellar pattern. Therefore, resorbed bone is replaced and the marrow spaces are filled with excessive fibrous connective tissue along with a dramatic increase in blood vessels, resulting in bone hypercellularity. Furtherly, bone hypercellularity may alleviate and the localized area change to a dense "pagetic bone," known as Paget's disease (https://en.wikipedia.org/ wiki /Paget%27s_disease_of_bone#cite_note-22).

1.1.4 Osteomalacia and rickets

Rickets is a condition that affects bone remodeling in children. It causes bone pain, poor growth and trouble sleeping, which can lead to bone deformities, such as: bowed legs, large forehead, bone fractures, an abnormally curved spine, or intellectual disability (https://rarediseases.info.nih.gov/diseases/5700/rickets; https://rarediseases. org/rare-diseases/rickets-vitamin-d-deficiency/). 2005. Retrieved 19 December 2017]. It usually occurs when children do not get enough vitamin D, which helps growing bones absorb important nutrients (http://www.nlm.nih.gov/ medlineplus/rickets.html). Whilst, adults can experience similar condition, which is known as osteomalacia. It is

caused by impaired bone metabolism mainly due to deficient levels of available calcium, phosphate, and vitamin D, or the resorption of calcium. The imperfection of bone metabolism causes inadequate bone mineralization, resulting in soft bone or fragile bones (Boukpessi et al., 2017 and Barros et al., 2013). Symptoms can include muscle weakness, body pains and fragility of the bones. In addition to inadequate levels of circulating mineral ions indispensable for bone and tooth mineralization, increase of mineralization-inhibiting proteins and peptides (such as osteopontin and acidic serine- and aspartate-rich motif peptides) in the extracellular matrix of bones and teeth contributs to matrix hypomineralization (osteomalacia) (Barros et al., 2013 and McKee et al., 2013 and Boukpessi et al., 2010).

In adults, osteomalacia is reversible, and treatment usually cures the problem within six months. Therefore, the deficient of bone growth caused by rickets may be arrested; causing permanent and irreversible skeletal deformities.

1.1.5 Fibrous dysplasia

Other than the most three common bone-mass deficient disease: osteoporosis, osteomalacia and rickets, fibrous dysplasia is a rare metabolic bone disease where normal bone and marrow is replaced with fibrous tissue, leading to weak formation of bone and prone to expansion, resulting in bone pains, bone deformities and pathologic fractures (DiCaprio et al., 2005). Fibrous dysplasia affects in monostotic or polyostotic way and may occur in isolation or in combination with café au lait skin macules and hyperfunctioning endocrinopathies, termed McCune–Albright syndrome;

or it may be associated with intramuscular myxomas, termed Mazabraud's syndrome, which is more rarely happens(Boyce et al., 2018 and Cabral et al., 1998).

Until now, treatment of fibrous dysplasia is mainly palliative, and is focused on managing fractures and preventing deformity. Intravenous bisphosphonates seems helpful to alleviate bone pain, therefore there is no clear evidence that they can cure bone lesions or prevent bone fractures (Plotkin et al., 2003 and Boyce et al., 2014). Surgical treatment of craniofacial skeleton frequently followed by post-operative fibrous dysplasia re-growth, so that surgical management is suggested to be focused on correction of functional deformities (Lee et al., 2012).

1.2 Osteoclastogenesis & RANKL/RANK/OPG system

The delicate balance of bone resorption and bone synthesis involved in bone remodeling is a physiological bone process that is regulated by osteoclasts and osteoblasts, respectively (Corral et al., 1998 and Karsenty et al., 2002). Excessive formation of osteoclasts is caused by usual activation of osteoclastogenesis, resulting in bone destruction and inflammation. A human osteoclast on bone is a large multinucleated cell and typically has five nuclei and is 150–200 μm in diameter. While, very large cells that may have dozens of nuclei occurs when macrophages convert into osteoclasts by cytokines (Basle et al., 1988 and Jain et al., 2009)

RANKL, a member of the tumor necrosis factor family, is produced by osteoblast and bone marrow stromal cells (Kong et al., 1999 and Yasuda et al., 1998),

and plays a crucial role in osteoclastogenesis (Hsu et al., 1999). Osteoclastogenesis progress through multiple stages, including differentiation, fusion, and activation (maturation) related by various factors, including cytokines, hormones and other cells in the bone microenvironment (Liu et al., 2009) (Figure 1).

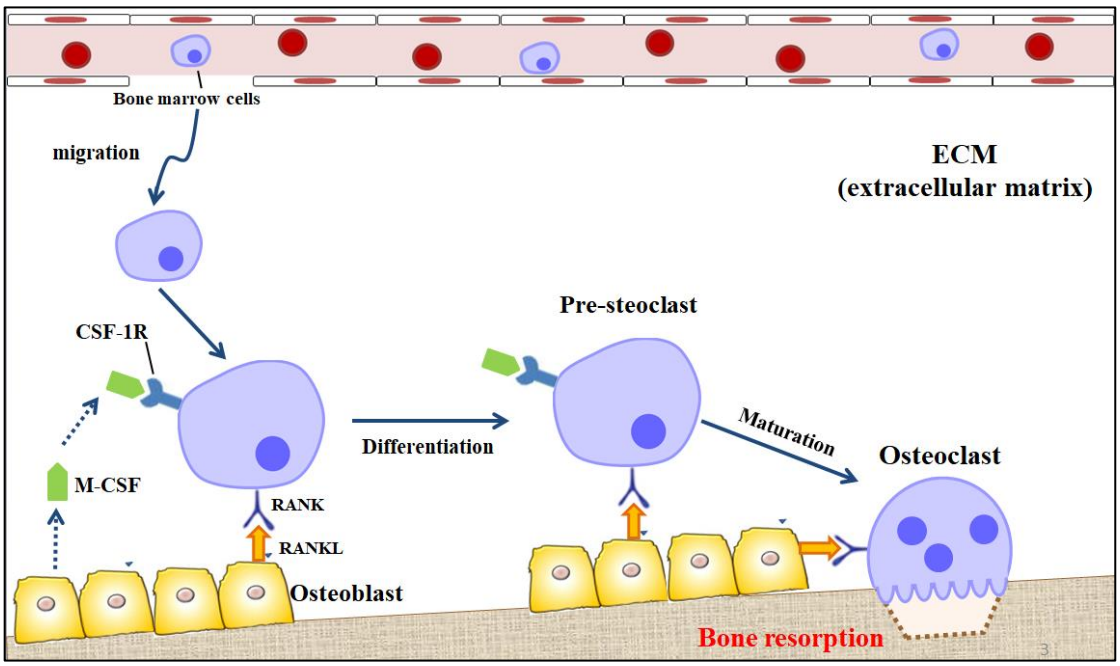

Figure 1.1 RANKL-induced osteoclast differentiation and muturation

RANKL (receptor activator of NF-ƙB ligand) and M-CSF (macrophage colony-stimulating factor) are necessary signals for osteoclast differentiation in bone marrow-derived macrophage precursor cells (Darnay et al., 1998 and Wada et al., 2006). Binding of M-CSF to c-Fms (colony-stimulating factor-q receptor) stimulates ERK and PI3K/Akt pathways which are involved in cell proliferation and survival (Ross, 2006); however, many studies show that M-CSF is not essential for RAW cell induced osteoclastogenesis (Lu et al., 2015 and Miyamoto et al., 2009).

The downstream intracellular signaling of RANKL-induced osteoclastogenesis, including TRAF6 (TNF receptor-associated factor 6)-dependent activation of NF-ƙB via the IƙB kinase complex and MAPKs (mitogen-activated protein kinases) such as ERK (extracellular signal–regulated kinases), p38 MAPK, and JNK (c-jun N-terminal kinase) (Teitelbaum et al., 2003 and Darnay et al., 1998 and Yamashita et al., 2007), is mediated by RANK (receptor activator of NF-ƙB) (Figure 2). TRAF6 binds to RANK-RANKL complex and then stimulates the activation of the JNK and NF-ƙB pathways which trigger the production of key transcription factors for osteoclastogenesis, including NFATc1 and c-Fos (Takayanagi et al., 2007 and Ishida et al., 2002 and Mohamed et al., 2007). Moreover, OPG (osteoprotegerin) acts as a decoy receptor by blocking RANKL binding to its cellular receptor RANK. The overexpression of OPG in osteoblasts blocks osteoclast production in mice and lead to osteopetrosis, whereas OPG-deficient mice results in osteoporosis (Wagner et al., 2001 and Simonet et al., 1997).

Thus, RANK/RANKL/OPG system is crucial signaling pathway that keeps the delicate balance between bone destruction and bone formation. Besides, other regulators such as IL-6, estrogens, vitamin D also involved in osteoclastogenesis regulation.

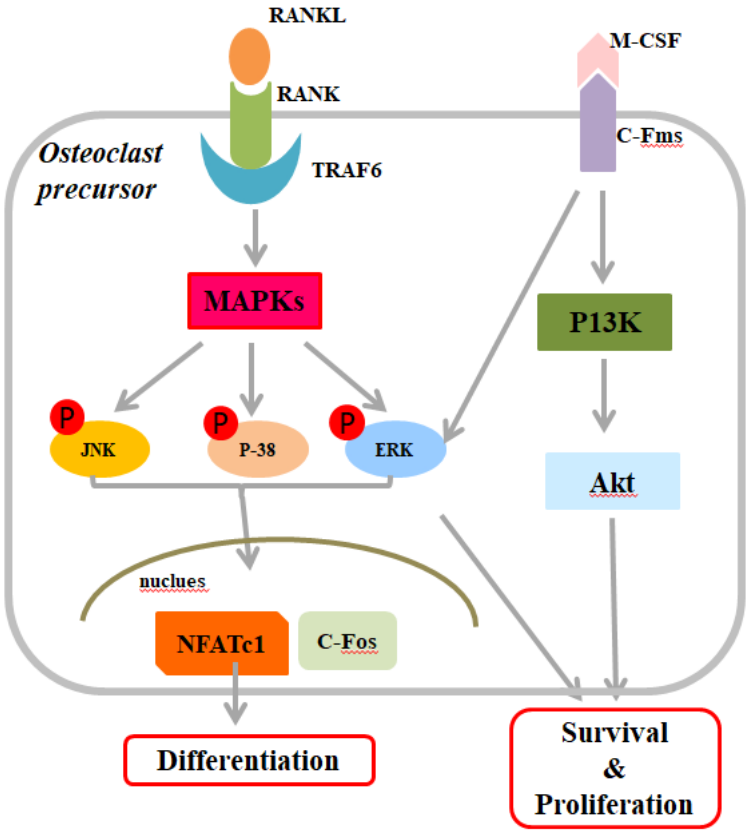

Figure 1.2 Downstream intracellular signaling way of RANKL-induced osteoclastogenesis

1.3 Therapeutic osteoclast inhibitors

1.3.1 Bisphosphonates

Bisphosphonates decrease bone resorption and increase mineralization by inhibiting osteoclast activity. Bisphosphonates directly effect on osteoclasts apoptosis, affect their differentiation and maturation and prevent bone resorption (Gralow et al., 2009 and Rodan et al., 1996).

First generation bisphosphonates are etidronate and clodronate, while

pamidronate and zoledronic acid (ZA) are second and third generations respectively (Carlin et al., 2000). The first and second generation bisphosphonates likely to prevent worsening of perifirmance status with high incidence of gastrointestinal side-effects and it is necessary for frequent dose adjustments, which may bring high risk of health problems (Dearnaley et al., 2003).

The third generation of bisphosphonates has been extensively examined in several clinical scenarios (Kozyrakis et al., 2018). Zoledronic acid is recommended over than other bisphosphonates for patients with bone metastases. Of the available bisphosphonates, zoledronic acid has the greatest efficacy shown to date (Rosen et al., 2001 and Palmieri et al., 2013).

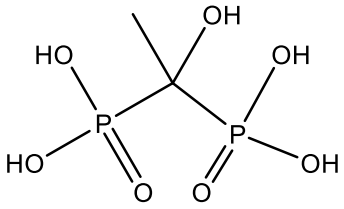

Etidronate

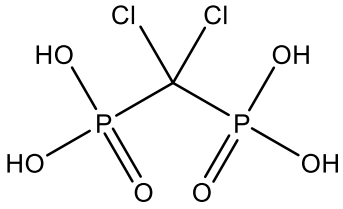

Clodronate

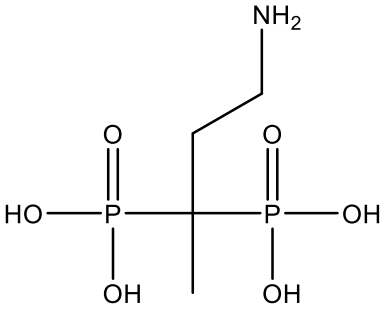

Pamidronate

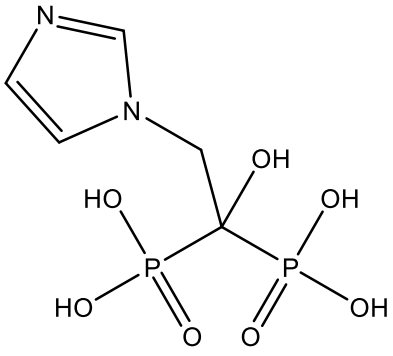

Zoledronic acid

Figure1.3 Four bisphosphonates: currently used osteoclast-inhibitors

1.3.2 Denosumab

Denosumab (DEN) a human monoclonal antibody against RANKL, so that it can inhibit bone resorption and prevent the bone destruction process by targeting RANKL (Muralidharan et al., 2013). It is effectively reduces the risk of first and subsequent SREs in patients.

The safety of DEN is different from that of bisphosphonates, particularly ZA, which have been associated with renal failure and jaw osteonecrosis (Cathomas et al., 2014). Jaw osteonecrosis and hypocalcemia caused by DEN are rare, rates up to 5% and 2%, respectively, which is much lower compare to that caused by bisphophonate agents (Smith et al., 2012).

1.4 Background of this research

To date, the administration of metabolic bone loss is mainly included two types: bisphosphonates and denosumab, which usually cause side-effects or even worse health problems in long-term use. Natural products have been studies over 100 years for not pharmaceutical products and drugs. Especially, folk medicine has an advantage over other natural products because of its long-and safe-use history. For these reasons, we attempts to evaluate the anti-osteoclastogenesis activity use natural-source plants, which might provide new effective drugs or clinical candidates for treatment of metabolic bone disease, such as osteoporosis, rheumatoid arthritis, Paget' disease and other skeletal-related events.

1.5 Objective of this research

Therefore, the objectives of this research are summarized as follow:

1. To screen 10 species of medicinal plants on osteoclastogenesis inhibitory activity and cell viability

2. To isolate and purity the chemical constituents the most effective crude extract and elucidate the structures of isolated compounds by spectroscopic techniques.

3. To evaluate the anti-osteoclastogenesis activity and cell viability of the isolated compounds.

4. To evaluate 19 commercial flavonoids and study on their structure-activity relationship (SAR)

Chapter 2

Evaluation of anti-osteoclastogenesis activity by Dragon's Blood (*Draco Daemonorops*)

2.1 Introduction

Osteoporosis is a chronic progressive bone disease which is affecting 75 million patients in the United States, Europe, and Japan alone. Annually, it causes more than 8.9 million fractures worldwide. In China, 88 million patients have been estimated to have initial osteoporosis, characterized by low bone mass and micro-architectural destruction of bone tissue (Lei et al., 2006).

Basically, osteoporosis has been divided into 4 types: Type I (postmenopausal osteoporosis), Type II (senile osteoporosis due to calcium deficiency in over-70-year-old people), Type III (triggered by disease or drugs, including endocrine osteoporosis, nutritional deficiency osteoporosis, drug-induced osteoporosis, renal osteoporosis, etc), and Type IV(idiopathic juvenile osteoporosis, which is more common in 8–14year old children associated with genetic link, is more frequent in females than males) (Zhao et al., 2012)

Medicinal plants are the backbone of traditional medicine; more than 3.3 billion people in the less developed countries utilize medicinal plants on a regular basis (Davidson-Hunt et al., 2000). *Epimedium* is a low-growing, deciduous, perennial plant, which are the most frequently used herb drugs in anti-osteoporotic Chinese traditional medicine formula (Zhang et al., 2006). Some researches displayed that *Herba Epimedii*, the dried leaf of *Epimedium* and its extracts have effect on stimulation of the osteoblastogenesis and suppression of the activity of osteoclasts (Zhang et al., 2012 and Hsieh et al., 2010).

In preliminary screening, investigation of 10 species of medicinal plants (shown in Figure 2.1). including *Murraya paniculata* (S1), *Guazuma ulmifolia* (S2), *Orthosiphon aristatus* (S3), *Sinapis arvensis* (S4), *Syzyguim polyanthum* (S5), *Andrographis paniculata* (S6), *Zingiber purpureum* (S7), *Kaempferia galangal* (S8), *Zingiber officinale* (S9), *Daemonorops draco* (S10) on RANKL-induced osteoclastogenesis in macrophages RAW 264.7 were performed.

The results of crude extracts are shown in Figure 2.2. In this state, the methanol extracts of *D. draco* display the most potent inhibitory activity at 100µg/ml and 10µg/ml with slight toxicity.

Figure 2.1 The 9 species of medicinal plants and DB powder (S9)

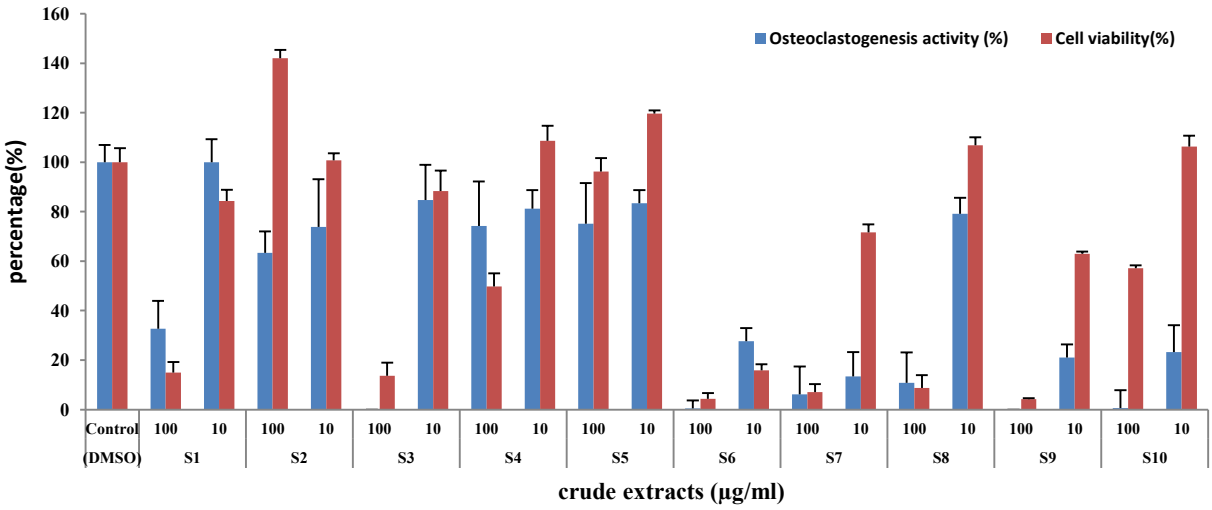

Figure 2.2 Screening of S1-S10 on anti-osteoclastogenesis activity and cell viability using macrophages RAW 264.7

Dragon's blood (DB) is a non-specific name for bright red resinous exudations which is obtained from different species of a number of distinct plant genera: *Dracaena* and *Daemonorops*, *Pterocarpus* and *Croton* (Gupta et al., 2008). In earliest history, DB was used as red color for painting as well as lacquer component, and has also been used for medicinal purposes for centuries (Gupta et al., 2008 and Harley et al., 1982). DB has high values for humans. Its antiviral, antibacterial and antifungal properties have been known since long time ago (Gupta et al., 2008). Besides, the antioxidant properties of its extract are cosmetically used in the production of anti-ageing skin creams. Studies also indicated that it has anti-cancer properties as wall (Rossi et al., 2003; Lopes et al., 2004; Gonzalez et al., 2006).

Daemonorops is a genus of rattan palms in the family Arecaceae found primarily in the tropics and subtropics of southeastern Asia with a few species extending into

southern China and the Himalayas (https://en.wikipedia.org/wiki/Daemonorops _draco). In particular, *Daemonorops draco*, an evergreen climbing palm producing a cluster of unbranched stems up to 15 meters long that climb into the surrounding vegetation, is the most well-known specie for producing valuable red resin. However, few studies have been issued that DB may alleviate bone destruction and bone cancer pain (Bao et al., 2015). Therefore, this study was designed to investigate the inhibition of RANKL-induced osteoclastogenesis activity by isolated metabolites from *D. draco*. Also, a number of commercially available flavonoids were used on anti-osteoclastogenesis evaluation to gain information on the structure-activity relationship (SAR).

Taxonomy of Daemonorops draco is classifies as: Kingdom: Plante; Family: Acrecaceae; Genus: Daemonorops; Species: draco.

2.2 Material and Method

2.2.1 General

Nuclear maganetic resonace (NMR) spectra were measured in chloroform-d and acetone-d6 using JEOL EC600 MHz NMR (JEOL, Tokyo, Japan). Matrix-assisted laser desorption/ionization time-of-flight mass spectrometry (MALDI-TOF-MS) spectra were determined using a Shimadzu AXIMA-Resonance spectrometer (Kyoto, Japan). Optical rotations were measured on a JASCO P-2300 spectropolarimeter (JASCO, Easton, MD, USA) equipped with a 10 cm path-length cell. Preparative

high-performance liquid chromatography (HPLC; Shimadzu LC-6AD) was performed using an Inertsil ODS-3 column (20mmø× 250mmL; GL sciences, Tokyo, Japan) .Silica gel (BW-200, Chromatotex, Japan) and Sephadex LH-20 (10-111μm, GE Healthcare) were used for open-column chromatography. Analytical thin layer chromatography (TLC) was performed on pre-coated silica gel 60 F_{254} glass plates (Merck, Germany). Osteoclasts were observed using fluorescence microscope (BZ-X710, KEYENCE, Japan)

2.2.2 Reagents

All reagents used in this study were showed as follow:

- FBS (Wako, biosera:CatNO.FB-1280/500/Lot NO.11824)
- KCl (Nacalai tesque, 285-14)
- KH_2PO_4 (Wako, 197-09075)
- $Na_2HPO_4 \cdot 12H_2O$ (Nacalai tesque, 31723-35)
- NaCl (Wako, 191-01665)
- 0.25%Trypsin-EDTA (Gibco, 25200)
- NEAA (Wako, 139-15651)
- Thiazolyl Blue Tetrazolium Bromide 98% (SIGMA-ALDRICH, M2128-500MG)
- Penicillin G (Wako, 598-08931)
- Streptomycin (Wako, 593-11291)
- MEM-α (with phenol red) (Wako, 135-15175)

- sRANKL (Oriental Yeast co., ltd. Cat NO.47187000/Lot NO.99204602)
- Mouse RAW 264.7 (Riken BRC, NO.RBRC-RCB0535, LotNO.040)
- Naphthol AS-MX phosphate disodium (Sigma-Aldrich, Lot NO.BCBT0082)
- Fast red violet LB salt (Sigma-Aldrich,Lot# MKBQ1481V)
- Sodium acetate, Anhydrous (Kishida, Lot NO. L47439L)
- Sodium tartrate Dihydrate (Nacalai tesque, Inc. Kyoto, Japan. Lot NO. MoM6858)
- Oleic acid (Nacalai tesque, Inc. Kyoto, Japan. Lot NO. M8B4013)
- 3.7% paraformaldehyde phosphate buffer (Wako, 161-20141)

2.2.3 Plant material

D. draco was provided by Prof. Irmanida Batubara, Department of Chemistry, Faculty of Mathematics and Natural Scien Bogor Agriculture University, Bogor, Indonesia.

2.2.4 Isolation and purification of *D. draco*

Powders of *D.draco* (289g) were extracted three times with methanol (MeOH) at room temperature. The solvent were removed under reduced pressure to give the MeOH extract (10g).

The MeOH extracts (5319mg) was subjected to open silica gel column chromatography and eluted with benzene/MeOH (7:3, 2.0ml/min) to give 7 fractions (Fr.1~7). Fr.1 was then subjected on preparative HPLC (Inertsil ODS-3,

20mmø× 250mmL) with gradient condition MeOH/H_2O (80:20-100:0, 60min) to give (2S)-5,7-dimethoxy-6-methylflavan (**1**, 7.1mg). Fr.2 was separated over Sephadex LH-20 using chloroform/MeOH (1:1, 1.0ml/min) to obtain 6 fractions (Fr.2-1~2-6). Fr.2-1 and fr.2-3 were subjected to preparative HPLC (Inertsil ODS-3, 20mmø× 250mmL) with the gradient condition MeOH/H_2O (80:20-100:0, 60min) and MeOH/H_2O (80:20-81:19, 40min) respectively and then yield to (2S)-5,7-dimethoxy-6-methylflavan (**1**, 51.6mg) again and (2S)-5-methoxy -6-methylflavan-7-ol (**2**, 13.1mg); besides, fr.2-6 was separated over silica gel column chromatography using chloroform/Acetone (7:3-6:4-5:5, 1.0ml/min) and furtherly subjected to preparative HPLC with (Inertsil ODS-3, 20mmø× 250mmL) with the gradient condition MeOH/H_2O (50:50-100:0, 40min) to give 3-(4-hydroxy-6-((2-(4-hydroxyphenyl)-5-methoxy-6-methylchroman-7-yl)oxy)-2-met hoxy-3-methylphenyl)-1-phenylpropan-1-one (**4**, 9.1mg). Moreover, fr.4 was subjected to Sephadex LH-20 using chloroform/MeOH (5:5-2:8, 1.2ml/min) and further purified by preparative HPLC (Inertsil ODS-3, 20mmø× 250mmL) with the gradient condition MeOH/H_2O (10:90-60:40, 40min) to yield 4-hydroxybenzoic acid (**3**, 37.8mg) again and afzelechin (**6**, 3.1mg). Fr.5 was separated over Sephadex LH-20 using EtOH/H_2O (10:0-8.5:1.5, 1.0ml/min) and further purified by preparative HPLC (Inertsil ODS-3, 20mmø× 250mmL) with the gradient condition MeOH/H_2O (5:95-100:0, 40min) to yield 3,4-dihydroxybenzoic acid (**5**, 33.1mg).

2.2.5 Cell subculture and Biological assays

The murine macrophage RAW264.7 cell line was purchased from Riken BRC (Japan) cultured in MEM-α supplied with 100U/ml of penicillin, 100U/ml of streptomycin 10%, 1% NEAA and 10% FBS. The cells were incubated at 37℃ in humidified atmosphere of 5% CO_2 on 10cm petri dish. 0.25%-EDAT (5ml) was added after cells were washed by 10mM PBS solution and incubated for 8min (37℃, 5% CO_2). Then, medium (5ml) was added and cell suspension was collected and centrifuged at 1000rpm for 1min, and fresh medium was added after removing the supernatant. Cell suspension was diluted to 1×10^5 cell/ml and incubated for next generation. Subculture was performed 2 times/week.

2.2.5.1 Anti-osteoclastogenesis activity

As shown in figure 2.3, anti-osteoclastogenesis activity evaluation was performed in 96-well plate at a density of 6×10^3 cells/well supplied with 100ng/ml RANKL solution. After 24h incubation, the adherent cells were co-cultured with RANKL (100ng/ml) and sample solutions (50, 100μg/ml) in refreshed medium. Samples were dissolved in DMSO and added into each well. The cells were incubated for 4 days and the medium was refreshed every 2 days with RANKL and sample solutions. Oleic acid (50μg/ml) was used as a positive control (Tan et al., 2014). In order to determine the number of osteoclasts and the number of nuclei per osteoclast at the end of incubation, cell were fixed by 3.7% paraformaldehyde phosphate buffer solution for 20min and then stained with TRAP staining solution containing 5 mg Naphthol AS-MX Phosphate, 500mLN-N-Dimethylformamide and 30 mg Fast Red

Violett LB Salt in 50 mL TRAP buffer (40 mM sodium-acetate and 10 mM sodium-tartrate in PBS) for 60 min. Cells with a positive staining for TRAP containing 3 or more nuclei were counted as osteoclasts. For quantification, the number of TRAP-positive multinucleated cells in each well was counted by the average number of five representative fields of view (magnification 100×) using electronic microscope (Keller et al., 2012; Vincent et al., 2009 and Collin et al., 2003). Osteoclastogenesis activity was calculated as a percentage of that measured in control treated with DMSO and RANKL solution only.

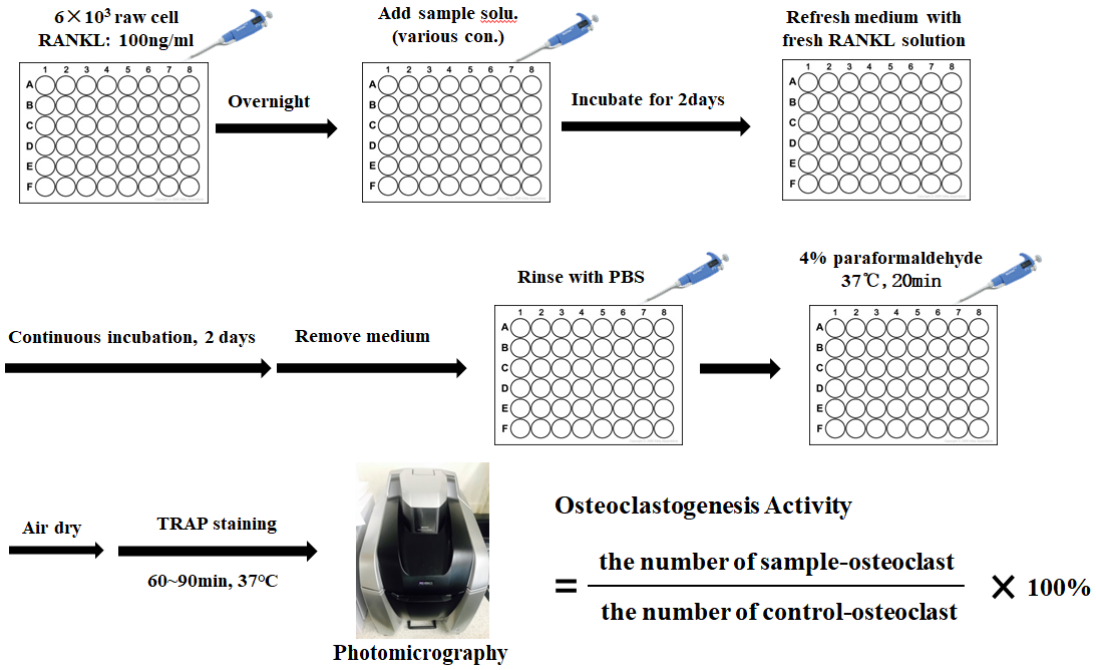

Figure 2.3 Anti-osteoclastogenesis activity evaluation

2.2.5.2 Cell viability measurement by MTT assay

Cell viability evaluation were performed in 24-well plate at a density of 5×10^4 cells/well. After 48h with varying concentrations of testing sample solutions, 50μl of

MMT solution was added to each well and incubated for additional 4h. Then the medium was removed, 1.0ml of isopropyl alcohol (containing 0.04N HCL) was added to each well to dissolve formazan crystals and 150μl transferred to a 96-well plate. The absorbance was measured at 590nm using microplate reader. Cell viability was calculated as a percentage of the viability measured in control cells treated with DMSO and without samples.

2.2.6 Statistical assay

All experiments were performed in triplicate (n=3) and data are expressed as mean values and standard deviation. A p-value of *$p<0.05$ and **<0.01 were considered statistically significance.

2.3 Results and discussion

2.3.1 Isolated compounds (1-6) from *D. draco*

To isolated active components, several times of silica gel and Sephadex LH-20 column chromatography, and C-18 reverse phase HPLC to obtain 4 flavonoids and 2 benzoic acid deriviates (**1-6**) (Figure 2.4).Among them, compound **(1)** and compound **(4)** were identified as novel compounds. All compounds were identified by NMR spectra and MALDI-TOF-MS and known compounds were furtherly confirmed by comparing to 1D NMR date in references.

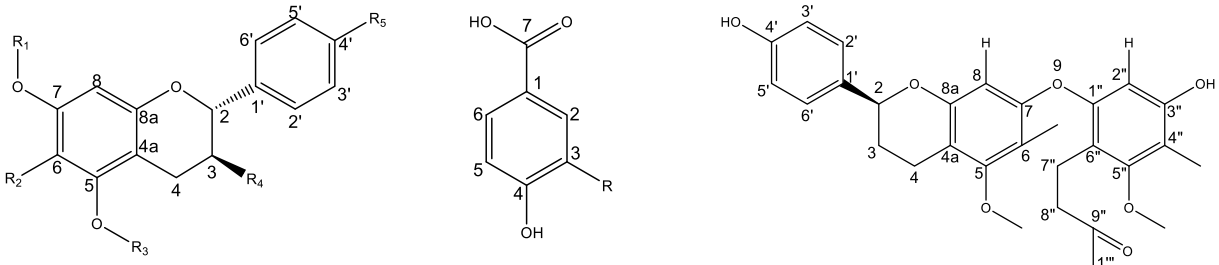

1: R_1=R_2=R_3=CH_3, R_4=R_5=H
2: R_1=H, R_2=R_3=CH_3, R_4=R_5=H
6: R_1=R_2=R_3=H, R_4=R_5=OH

3: R= H
5: R=OH

4

Figure 2.4 Isolated compounds from *D.draco*

2.3.1.1 Identification of isolation compounds 1-6

(2S)-5,7-dimethoxy-6-methylflavan (1) was obtained as yellow crystal and determined to have molecular formula $C_{18}H_{20}O_3$ by MALDI-TOF-MS (positive ion mode) m/z: 285.1138 $[M+H]^+$, implying 9 degrees of unsaturation; optical rotation measurement (JASCO P-2300 system): $[\alpha]_D^{20}$-3.50 (c 0.3, $CHCl_3$). Optical rotation of **1** was compared to that of **2,** indicated that **1** has the same **(2S)** configuration as **2**. Combined analysis of the 1H and 13C NMR (Table 1) plus the HMQC spectroscopic data revealed the presence three singlet regarding one methyl and two methoxy groups (δ_H 2.09, δ_H 3.71 and δ_H 3.76), two sp^3 methylenes, one oxymethine, six aromatic protons (δ_H 6.30, δ_H 7.41, δ_H 6.70 and δ_H 7.31). These data accounted for all NMR resonances of **1** and four of the nine unsaturations, indicating that **1** include two aromatic rings. Analysis of 1H-1H COSY spectrum established one partial structure of H-2/H_2-3 and H_2-3/ H_2-4. According to the HMBC spectrum of compound **5**, long-range correlations were observed between H-2 and C-4, C-1',C-2' and C-6'; H_2-4 and C-2, C-3 C-5, C-4a and C-8a; H-6-Me and C-6 and C-7; H-7-OMe and C-7;

H-5-OMe and C-5; H-8 and C-4a, C-7, C-6 and C-8a; H-4' and C-2'and C-6'; H-3'/5' and C-1'; H-2'/6' and C-4' (Figure 2). And NOESY data shows the correlations between H-5-OMe and H_2-4, H-6-Me; H-7-OMe and H-8; H-2'/6' and H_2-3 (Figure 3). Thus, compound **1** was identified as (2S)-5,7-dimethoxy-6-methylflavan, a novel compound.

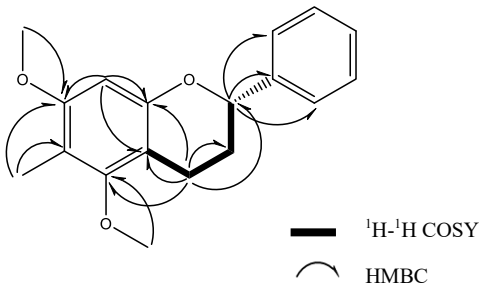

Figure 2.5 1H-1H COSY and HMBC correlations of **1**

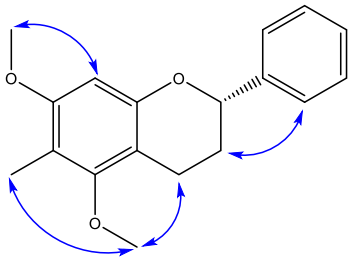

Figure 2.6 Selected NOESY correlations of **1**

Table 2.1 ^{1}H and ^{13}C NMR data of compound **1**

Position	δ_H (ppm)	J(Hz)	δ_C (ppm)
2	4.99dd	2.04, 10.32	77.92
3	1.98-2.05m		29.86
	2.18-2.21m		
4	2.75-2.87m		19.84
4a			107.55
5			157.15
6			111.47
7			157.50
8	6.30s		95.78
8a			154.06
1’			141.80
2’,6’	7.41m		126.12
3’,5’	7.38m		128.60
4’	7.31dd	2.04, 7.56	127.95
5-OMe	3.71s		55.63
6-Me	2.09s		8.57
7-OMe	3.76s		60.09

NMR data were measured in $CDCl_3$.

(2S)-5-methoxy-6-methylflavan-7-ol (2) was obtained as colorless crystal and determined to have molecular formula $C_{17}H_{18}O_3$ by MALDI-TOF-MS (positive ion mode) m/z: 271.5289 $[M+H]^+$, implying 9 degrees of unsaturation; optical rotation measurement (JASCO P-2300 system): $[\alpha]_D^{20}$-9.30 (c 2.1, $CHCl_3$). ^{1}H NMR spectrum ($CDCl_3$, 600MHz): δ (ppm) 1.99-2.01 (1H, m,H-3), 2.17-2.20 (1H, m,H-3), 2.12 (3H, s, H-6-Me), 2.76-2,81 (2H, m, H-4), 3.71 (3H, s, H-5-OMe), 4.65 (1H, s, H-7-OH), 4.97 (1H, dd, J=2.04, 9.96 Hz, H-2), 6.22 (1H, s, H-8), 7.31 (1H, dd, J= 2.04, 7.56 Hz, H-4’), 7.37 (2H, m, H-2’,6’), 7.39 (2H, m, H-3’,5’); ^{13}C NMR spectrum ($CDCl_3$, 150MHz): δ (ppm) 19.84(C-4), 29.86(C-3), 55.63(C-5-OMe), 60.09(C-6-Me), 77,92(C-2), 95.78(C-8), 107.55(C-4a), 111.47(C-7), 126.12(C-2’,6’), 127.95(C-4’),

128.60(C-3',5'), 141.80(C-1'), 154.06(C-8a), 157.15(C-6), 157.50(C-5). Spectral data were coincided to that of published report (Cardillo et al., 1971).

4-hydroxybenzoic acid (3) was obtained as colorless solid and determined to have molecular formula $C_7H_6O_3$ by MALDI-TOF-MS (positive ion mode) m/z: 139.1261 $[M+H]^+$, implying 5 degrees of unsaturation.^{1}H NMR spectrum ($CDCl_3$, 600MHz): δ (ppm) 6.79-6.80 (2H, d, J=8.22 Hz, H-3,5), 7.85-7.86 (2H, d, J=8.94 Hz, H-2,6); ^{13}C NMR spectrum ($CDCl_3$, 150MHz): δ (ppm) 114.70(C-3,5), 121.40(C-1), 131.68(C-2,6), 162.01(C-4), 168.84(C-7). Spectral data were coincided to that of published report (Sukari et al., 2013).

(2R)-3-(4-hydroxy-6-((2-(4-hydroxyphenyl)-5-methoxy-6-methylchroman-7-yl)oxy)-2-methoxy-3-methylphenyl)-1-phenylpropan-1-one (4) was obtained as brown crystal and determined to have molecular formula $C_{34}H_{34}O_7$ by MALDI-TOF-MS (positive ion mode) m/z: 577.1743 $[M+Na]^+$, implying 18 degrees of unsaturation; optical rotation measurement (JASCO P-2300 system): $[\alpha]_D^{20}$ +6.6233 (c 0.6, $CHCl_3$). Combined analysis of the ^{1}H and ^{13}C NMR (Table 2) plus the HMQC spectroscopic data revealed the presence three singlet regarding two methyls and two methoxy groups (δ_H 2.10, δ_H 2.07, δ_H 3.70 and δ_H 3.74), four sp^3 methylenes, one oxymethine, eleven aromatic protons (δ_H 6.20, δ_H 6.26, δ_H 6.83, δ_H 7.23, δ_H 7.41, δ_H 7.54, and δ_H 7.96), as well as twenty-four aromatic carbons and one ketone carbon (δ_C 203.07). These data accounted for all NMR resonances of **4** and sixteen of the eighteen unsaturations, indicating that **4** include four aromatic rings. Analysis of

1H-1H COSY spectrum established several partial structures: H_2-3/H_2-4 and H_2-3/H-2, H-7''/H-8'', H-(3', 5')/H-(2', 6') as well as H-(3''', 5''')/H-(2''', 6''') and H-(3''', 5''')/H-4'''(Figure 2). According to the HMBC spectrum of compound 5, long-range correlations were indicated as follows: (Figure 2). And NOESY data shows the correlations between H-2'/6' and H-2, H-2'/6' and H-3, H-2 and H-4, H-4 and H-5-OMe and H-8'', H-8'' and H-2''/6'' (Figure 3). Thus, compound **4** was identified as3-(4-hydroxy-6-((2-(4-hydroxyphenyl)-5-methoxy-6-methylchroman-7-yl)oxy)-2-methoxy-3-methylphenyl)-1-phenylpropan-1-one, a novel compound.

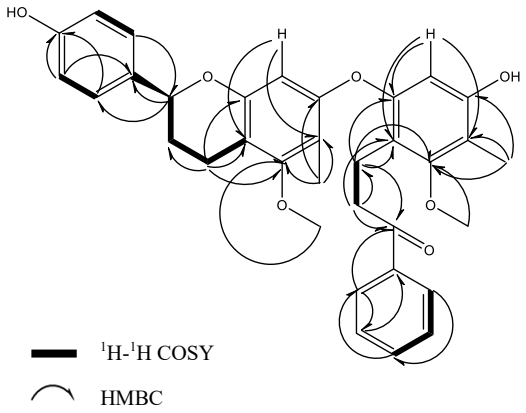

Figure 2.7 1H-1H COSY and HMBC correlations of **4**

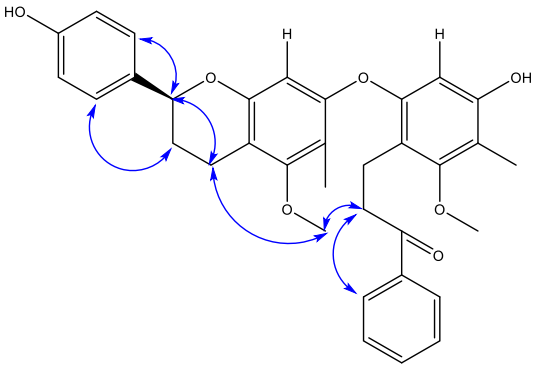

Figure 2.8 Selected NOESY correlations of **4**

Table 2.2 ^{1}H and ^{13}C NMR data of compound **4**

Position	δ_H (ppm)	J(Hz)	δ_C (ppm)
2	4.88dd	2.04,8.00	77.56
3	1.92-2.00m		29.67
	2.12-2.15m		
4	2.70-2.83m		20.00
5			157.32
6			109.51
7			153.77
8	6.20s		99.55
4a			107.77
8a			154.16
1’			133.49
2’,6’	7.23d	9.66	127.62
3’,5’	6.83d	8.22	115.48
4’			156.01
1”			153.66
2”	6.26s		100.78
3”			154.33
4”			109.40
5”			158.22
6”			113.54
7”	2.93t	6.18	17.35
8”	3.41t	6.18	39.99
9”			203.07
1”’			136.23
2”’,6”’	7.96d	7.56	128.47
3”’,5”’	7.41d	8.22	128.68
4”’	7.54d	7.56	133.80
5-OMe	3.70s		60.05
6-Me	2.10s		8.48
4”-Me	2.07s		8.93
5”-OMe	3.74s		60.64

NMR data were measured in $CDCl_3$

3,4-dihydroxybenzoic acid (5) was obtained as colorless solid and determined to have molecular formula $C_7H_6O_4$ by MALDI-TOF-MS (positive ion mode) m/z: 154.8848 $[M+H]^+$, implying 5 degrees of unsaturation.^{1}H NMR spectrum ($CDCl_3$,

600MHz): δ (ppm) 6.76-6.78 (1H, d, J=7.56 Hz, H-6), 7.39-7.41 (1H, dd, J=2.04, 3.45 Hz, H-5), 7.41-7.42 (1H, d, J=2.04 Hz, H-2); ^{13}C NMR spectrum ($CDCl_3$, 150MHz): δ (ppm) 114.46(C-6), 116.40(C-2), 121.78(C-1), 122.61(C-5), 144.71(C-3), 150.19(C-4), 168.93(C-7). Spectral data were coincided to that of published report (Syafni et al., 2012).

(+)-Afzelechin (6) was obtained as white crystal and determined to have molecular formula $C_{15}H_{14}O_5$ by MALDI-TOF-MS (positive ion mode) m/z: 275.0027 $[M+H]^+$, implying 9 degrees of unsaturation; optical rotation measurement (JASCO P-2300 system): $[\alpha]_D^{20}$ +0.52 (c 0.09, Acetone:EtOAc=9:1).^{1}H NMR spectrum (methanol-d4, 600MHz): δ (ppm) 2.48 (1H, dd, J=8.94, 16.17 Hz, H-4ax), 2.86 (1H, dd, J=5.46, 15.81Hz, H-4eq), 3.94-3.98 (1H, m, H-3), 4.57 (1H, d, J=7.56Hz, H-2), 5.81 (1H, d, J=2.04 Hz, H-6), 5.90 (1H, d, J=2.10 Hz, H-8), 6.76 (2H, d, J=8.94 Hz, H-3'/5'), 7.20 (2H, d, J=8.94 Hz, H-2'/6'); ^{13}C NMR spectrum (methanol-d4, 150MHz): δ (ppm) 27.59(C-4), 67.31(C-3), 81.54(C-2), 94.13(C-6), 94.95(C-8), 99.55(C-4a), 114.69(C-3',5'), 128.28(C-2',6'), 130.15(C-1'), 155.66(C-8a), 156.24(C-5), 156.53(C-7), 157.08(C-4'). Spectral data were coincided to that of published report (Saraswathy et al., 2012).

2.3.1.2 Anti-osteoclastogenesis activity and cell viability of isolated compounds 1-6

To evaluate the inhibition of RANKL-induced osteoclastogenesis activity of isolated compounds using macrophage RAW 264.7 cells. The cells were treated with

or without the isolated compounds at various concentrations supplied with 100ng/ml RANKL solution, and the osteolastogenesis activity was calculated as a percentage of that measured in control treated with DMSO and RANKL solution only. As shown in figure 2.9, com.1 was identified as a novel flavan compound and exhibited the most potent inhibition on osteoclastogenesis, remains only 22% osteoclastogenesis activity at 10μM without any cytotoxicity and no osteoclastogenesis activity at 100μM with 75% cell viability. Com.2 also showed fairly good inhibition on osteoclastogenesis, with only 50% osteoclastogenesis activity and no cytotoxicity at 10μM. Furtherly compared to positive control, both com.1 and com.2 exhibited more inhibition on osteoclastogenesis. Com.3 remained 25% osteoclastogenesis activity with no toxicity at 100μM; however, com.5 showed no osteoclastogenesis activity at all. Com.4 and com.6 showed slight inhibition, with 73% and 65% osteoclastogenesis activity respectively. Based on these results, the absent of 3-hydroxyl group of benzoic acid was important for anti-osteoclastogenesis activity. Moreover, the presence of 7-methoxy in flavan structure was crucial for anti-osteoclastogenesis; also, less methylation of flavonoid structure seems to provide weaker anti-osteoclastogenesis activity.

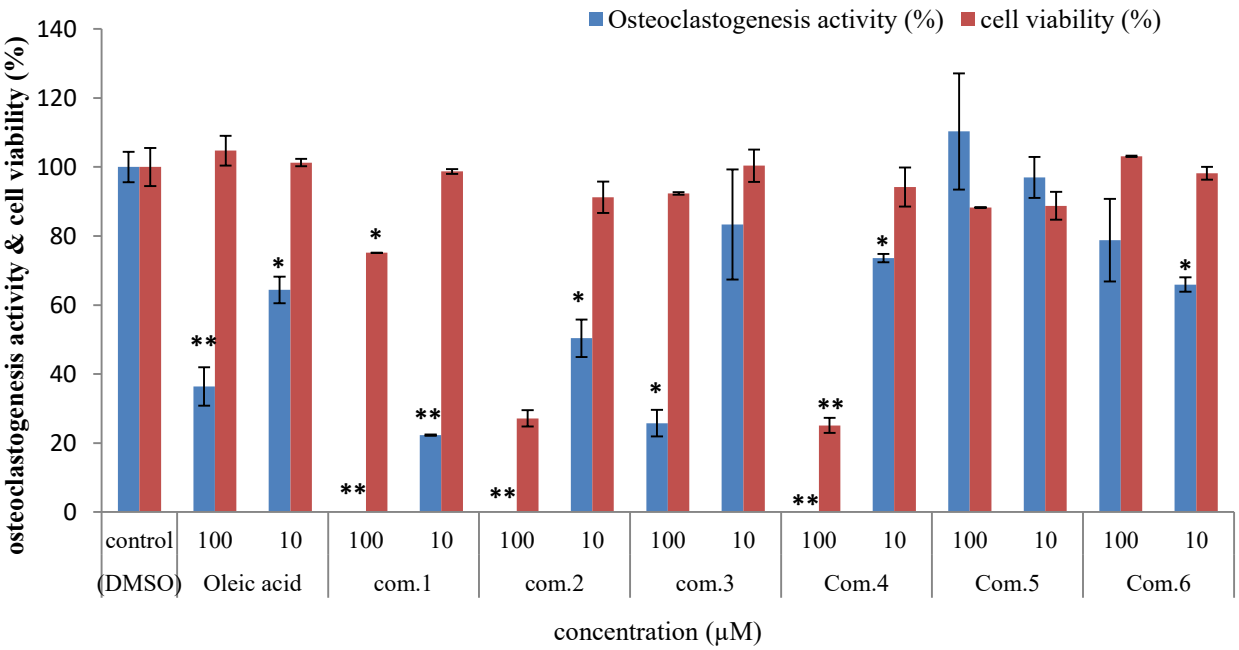

Figure 2.9 Osteoclastogenesis activity and cell viability of isolated compounds **1-6** (concentrations at 10/100μM). Assays were measured in triplet experiment. Each value is expressed as the mean ± SD of triplet determinations. *p < 0.05, **p < 0.01 versus the control group. (Control: DMSO; Oleic acid was used as positive control)

2.4 Conclusions

We studied the effect of six isolated compounds from *D. draco* on anti-osteoclastogenesis activity. (2S)-5,7-dimethoxy-6-methylflavan (1) as a novel compound displayed dramatically significant inhibition on osteoclastogenesis activity, which may provide potent candidates for anti-osteoclastogenesis drugs. The degrees of methylation of flavonoid structure likely to give more potent inhibition on osteoclastogenesis. This information gives us an idea to evaluate more flavonoid on anti-osteoclastogenesis activity to elucidate the structure-activity relations.

Chapter 3

Evaluation of anti-osteoclastogenesis activity by 19 commercial flavonoid.

3.1 Introduction

In chapter 2, compound **1** exhibited 100% inhibition and 78% inhibition on osteoclastogenesis at 100μM and 10μM respectively without significant cell cytotoxicity, which is much effective than that of positive control (64% inhibition and 34% inhibition at 100μM and 10μM respectively). Compound **2** displayed 50% inhibition on osteoclastogenesis 10μM without cytotoxicity, however, it showed quite significant cytotoxicity at 100μM. In comparison, the only difference between **1** and **2** is the methylation of 7-hydroxyl, indicating that 7-methoxy group provide more effective activity on osteoclastogenesis than 7-hydroxy gounp. These results were corresponded to data of compound **6**. Compound **6** exhibited only 35% inhibition on osteoclastogenesis.

Based on these results, we hypothesize that the degree of methylation in flavonoid skeleton might be important for anti-osteoclastogenesis; moreover, the absence of hydroxyl group at 3-position as well as in B ring may also provide more effect on anti-osteoclastogenesis activity.

To furtherly elucidate more information of SAR in flavonoid skeleton; nineteen commercial flavonoids were performed on anti-osteoclastogenesis activity.

3.2 Materials and methods

3.2.1 General

Nuclear maganetic resonace (NMR) spectra were measured in chloroform-d and acetone-d6 using JEOL EC600 MHz NMR (JEOL, Tokyo, Japan). Matrix-assisted laser desorption/ionization time-of-flight mass spectrometry (MALDI-TOF-MS) spectra were determined using a Shimadzu AXIMA-Resonance spectrometer (Kyoto, Japan). Optical rotations were measured on a JASCO P-1010 polarimeter (JASCO Corporation, Tokyo, Japan). Preparative high-performance liquid chromatography (HPLC; Shimadzu LC-6AD) was performed using an Inertsil ODS-3 column (20mmø× 250mmL; GL sciences, Tokyo, Japan) .Silica gel (BW-200, Chromatotex, Japan) and Sephadex LH-20 (10-111μm, GE Healthcare) was used for open-column chromatography. Analytical thin layer chromatography (TLC) was performed on pre-coated silica gel 60 F_{254} glass plates (Merck, Germany). Osteoclasts were observed using fluorescence microscope (BZ-X710, KEYENCE, Japan)

3.2.2 Reagents

All reagents used in this study were showed as follow:

- FBS (Wako, biosera:CatNO.FB-1280/500/Lot NO.11824)
- KCl (Nacalai tesque, 285-14)
- KH_2PO_4 (Wako, 197-09075)
- $Na_2HPO_4 \cdot 12H_2O$ (Nacalai tesque, 31723-35)

- NaCl (Wako, 191-01665)
- 0.25%Trypsin-EDTA (Gibco, 25200)
- NEAA (Wako, 139-15651)
- Thiazolyl Blue Tetrazolium Bromide 98% (SIGMA-ALDRICH, M2128-500MG)
- Penicillin G (Wako, 598-08931)
- Streptomycin (Wako, 593-11291)
- MEM-α (with phenol red) (Wako, 135-15175)
- sRANKL (Oriental Yeast co., ltd. Cat NO.47187000/Lot NO.99204602)
- Mouse RAW 264.7 (Riken BRC, NO.RBRC-RCB0535, LotNO.040)
- Naphthol AS-MX phosphate disodium (Sigma-Aldrich, Lot NO.BCBT0082)
- Fast red violet LB salt (Sigma-Aldrich,Lot# MKBQ1481V)
- Sodium acetate, Anhydrous (Kishida, Lot NO. L47439L)
- Sodium tartrate Dihydrate (Nacalai tesque, Inc. Kyoto, Japan. Lot NO. MoM6858)
- Oleic acid (Nacalai tesque, Inc. Kyoto, Japan. Lot NO. M8B4013)
- 3.7% paraformaldehyde phosphate buffer (Wako, 161-20141)

3.2.3 Commercial flavonoids

As we discussed in chapter 2, three flavonoids (**1, 2 and 6**) displayed anti-osteoclastogenesis activity and indicated that methylation may provide more inhibition effect on osteocoastogenesis than hydroxyls. Furtherly, nineteen

commercial flavonoids: **baicalein** (027-07751, Wako, Japan), **luteolin** (1125S, Extrasynthese, France), **kaempferol** (K0018, TCI, Tokyo, Japan), **quercetin·2H_2O** (177-00401, Wako, Japan), **myricetin** (Extrasynthese, France), **apigenin** (A9185, Aldrich Chemical Company Inc., Milwaukee, Wisconsin), **galangin** (06217TY, Aldrich Chemical Company Inc., Milwaukee, Wisconsin), **chrysin** (C-3018, Sigma Aldrich, USA), **taxifolin** (T-4512, Sigma Aldrich, USA), **3-hydroxyflavone** (H379, TCI, Tokyo, Japan), **7- hydroxyflavone** (H0852, TCI, Tokyo, Japan), **robinetin** (0069, Extrasynthese, France), **(-)-epicatechin** (E-1753,Sigma Aldrich, USA), **(-)-catechin** (035-18461, Wako, Japan), **flavone** (160-12, Nacalai Tesque, Inc., Kyoto, Japan), **flavanone** (Lot LY07708CX, Aldrich Chemical Company Inc., Milwaukee, Wisconsin), **morin (**C.I.Nr. 75660, Merck, Germany**)**, **naringenin** (241-33, Nacalai Tesque, Inc. Kyoto, Japan), and **hesperetin** (H-4125, Sigma Aldrich, USA), were used in this chapter to elucidate SAR of flavonoid skeleton on anti-osteoclastogenesis activity.

3.2.4 Cell subculture and Biological assay

The murine macrophage RAW264.7 cell line was purchased from Riken BRC (Japan) cultured in MEM-α supplied with 100U/ml of penicillin, 100U/ml of streptomycin 10%, 1% NEAA and 10% FBS. The cells were incubated at 37℃ in humidified atmosphere of 5% CO_2 on 10cm petri dish. 0.25%-EDAT (5ml) was added after cells were washed by 10mM PBS solution and incubated for 8min (37℃, 5% CO_2). Then, medium (5ml) was added and cell suspension was collected and

centrifuged at 1000rpm for 1min, and fresh medium was added after removing the supernatant. Cell suspension was diluted to 1×10^5 cell/ml and incubated for next generation. Subculture was performed 2 times/week.

3.2.4.1 Anti-osteoclastogenesis activity

Anti-osteoclastogenesis activity evaluation was performed in 96-well plate at a density of 6×10^3 cells/well supplied with 100ng/ml RANKL solution. After 24h incubation, the adherent cells were cocultured with RANKL (100ng/ml) and sample solutions (10μM) in refreshed medium. Samples were dissolved in DMSO and added into each well. The cells were incubated for 4 days and the medium was refreshed every 2 days with RANKL and sample solutions. Oleic acid (10μM) was used as a positive control (Tan et al., 2014). In order to determine the number of osteoclasts and the number of nuclei per osteoclast at the end of incubation, cell were fixed by 3.7% paraformaldehyde phosphate buffer solution for 20min and then stained with TRAP staining solution containing 5 mg Naphthol AS-MX Phosphate, 500mLN-N-Dimethylformamide and 30 mg Fast Red Violett LB Salt in 50 mL TRAP buffer (40 mM sodium-acetate and 10 mM sodium-tartrate in PBS) for 60 min. Cells with a positive staining for TRAP containing 3 or more nuclei were counted as osteoclasts. For quantification, the number of TRAP-positive multinucleated cells in each well was counted by the average number of five representative fields of view (magnification 100×) using electronic microscope (Keller et al., 2012; Vincent et al., 2009 and Collin et al., 2003). Osteoclastogenesis activity was calculated as a

percentage of that measured in control treated with DMSO and RANKL solution only.

3.2.4.2 Cell viability measurement by MTT assay

Cell viability evaluation was performed in 24-well plate at a density of 5×10^4 cells/well. After 48h with 10μM of testing sample solutions, 50μl of MTT solution was added to each well and incubated for additional 4h. Then the medium was removed, 1.0ml of isopropyl alcohol (containing 0.04N HCL) was added to each well to dissolve formazan crystals and 150μl transferred to a 96-well plate. The absorbance was measured at 590nm using microplate reader. Cell viability was calculated as a percentage of the viability measured in control cells treated with DMSO and without samples.

3.2.5 Statistical assay

All experiments were performed in triplicate (n=3) and data are expressed as mean values and standard deviation. A p-value of *$p<0.05$ and **<0.01 were considered statistically significance.

3.3 Results and discussion

Structural illustration of 19 commercial compounds was shown in Figure 3.1.

As shown in figure 3.2, compare baicalein （no cytoxicity, completed anti-osteoclastogenesis activity) to luteolin (50% cytotoxicity and 46% anti-osteoclastogenesis activity) and quercetin (27% cytotoxicity, 35% anti-osteoclastogenesis activity), it seems that hydroxyl groups on B-ring provide more cell toxicity and less osteoclastogenesis activity, indicating that the absence of hydroxyl groups on B-ring is important for anti-osteoclastogenesis activity.

Furtherly, compare baicalein (no cytotoxicity, completed anti-osteoclastogenesis activity) to galangin (no cytotoxicity, 73% anti-osteoclastogenesis activity) and chrysin (no toxicity, 52% anti-osteoclastogenesis activity) (shown in figure 3.3), it indicated that 6-hydroxyl group is more important than 3- hydroxyl group providing more effective inhibition on osteoclastogenesis. As discussed in chapter 2, comparison of com.1 (no cytotoxicity, 78% anti-osteoclastogenesis activity) and com.2 (no toxicity, 50% anti-osteoclastogenesis activity) indicated that 7-methoxyl group provide more anti-osteoclastogenesis activity than 7-hydroxy group, indicated that methylation might be important for anti-osteoclastogenesis activity.

As shown in figure 3.3 and figure 3.4, it shows no much difference between 3-hydroxyflavone, 7-hydroxyflavone, and flavone, all remains about 60%

osteoclstogenesis activity without any cytotoxicity, which indicated that neither 7-hydroxyl group nor 3-hydroxyl group could be important on anti-osteoclastogenesis activity in flavone skeleton.

Besides, as shown in figure 3.4, it was very interesting that we found (3R)-hydroxyl group provide much more effective activity on osteoclastogenesis inhibition than (3S)-hydroxyl group by comparing (-)-epicatechin (no cytotoxicity, 64% anti-osteoclastogenesis activity) and (-)-catechin (no cytotoxicity, 18% anti-osteoclastogenesis activity).

As shown in figure 3.3 and figure 3.5, it indicated that double bond at C2 and C3 position increase inhibition on osteoclastogenesis by comparing apigenin (slight cytotoxicity, 49% anti-osteoclastogenesi activity) and naringenin (no cytotoxicity, only 19% anti-osteoclastogenesis activity).

Cell viability and osteoclastogenesis activity of 19 commercial flavonoids were summarized in Table 3.1.

Moreover, this is the first report to study and develop an early SAR profile of flavonoid skeleton on anti-osteoclastogenesis activity, as summarized in Figure 3.7

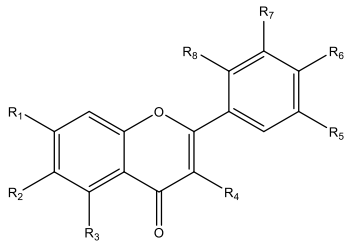

Baicalein: R_1=R_2=R_3=OH; R_2=R_5=R_6=R_7=R_8=H

Luteolin: R_1=R_3=R_6=R_7=OH; R_2=R_4=R_5=R_8=H

Kaempferol: R_1=R_3=R_4=R_6=OH; R_2=R_5=R_7=R_8=H

Quercetin: R_1=R_3=R_4=R_6=R_7=OH; R_2=R_5=R_8=H

Myricetin: R_1=R_3=R_4=R_5=R_6=R_7=OH; R_2=R_8=H

Apigenin: R_1=R_3=R_6=OH; R_2=R_4=R_5=R_7=R_8=H

Galangin: R_1=R_3=R_4=OH; R_2=R_5=R_6=R_7=R_8=H

Chrysin: R_1=R_3=OH; R_2=R_4=R_5=R_6=R_7=R_8=H

3-hydroxyflavone: R_4=OH; R_1=R_2=R_3=R_5=R_6=R_7=R_8=H

7-hydroxyflavone: R_1=OH; R_2=R_3=R_4=R_5=R_6=R_7=R_8=H

Robinetin: R_1=R_4=R_5=R_6=R_7=OH; R_2=R_3=R_8=H

Flavone: R_1=R_2=R_3=R_4=R_5=R_6=R_7=R_8=H

Morin: R_1=R_3=R_4=R_6=R_8=OH; R_2=R_5=R_7=H

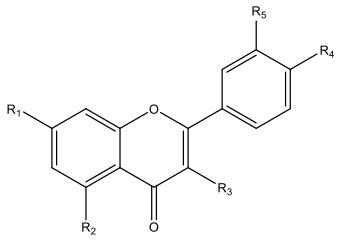

Taxifolin: R_1=R_2=R_3=R_4=R_5=OH

Naringenin: R_1=R_2=R_4=OH; R_3=R_5=H

Hesperetin: R_1=R_2=R_5=OH; R_4=OMe; R_3=H

Flavanone: R_1=R_2=R_3=R_4=R_5=H

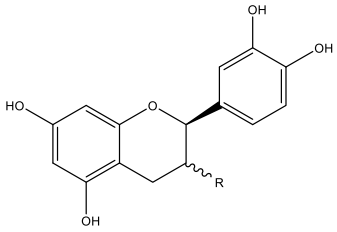

(-)-Epicatechin: R= OH

(-)-Catechin: R= OH

Figure 3.1 Structures of 19 commercial flavonoids

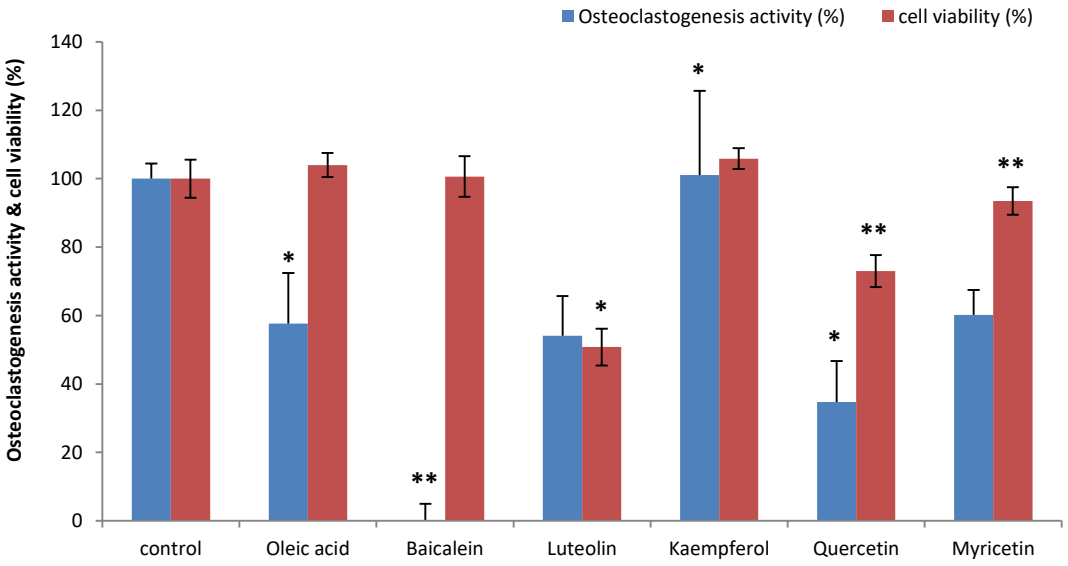

Figure 3.2 *Osteoclastogenesis activity and cell viability of commercial compounds: baicalein, luteolin, kaempferol, quercetin, and myricetin (10μM). Assays were measured in triplet experiment. Each value is expressed as the mean ± SD of triplet determinations. *p < 0.05, **p < 0.01 versus the control group. (Control: DMSO; Oleic acid was used as positive control)*

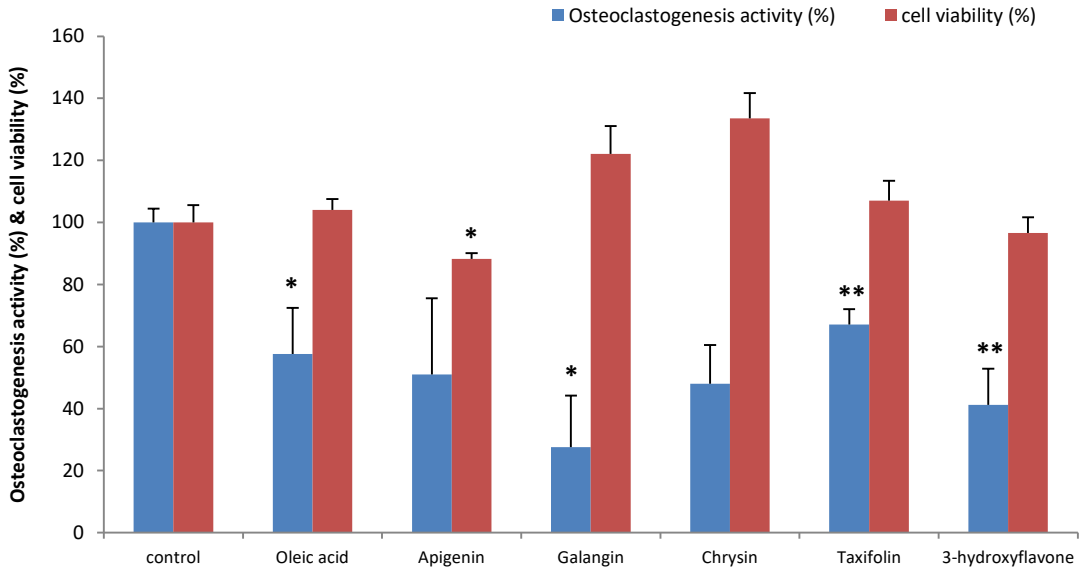

Figure 3.3 *Osteoclastogenesis activity and cell viability of commercial compounds: apigenin, galangin, chrysin, taxifolin and3-hydroxyflavone (10µM). Assays were measured in triplet experiment. Each value is expressed as the mean ± SD of triplet determinations. *p < 0.05, **p < 0.01 versus the control group. (Control: DMSO; Oleic acid was used as positive control)*

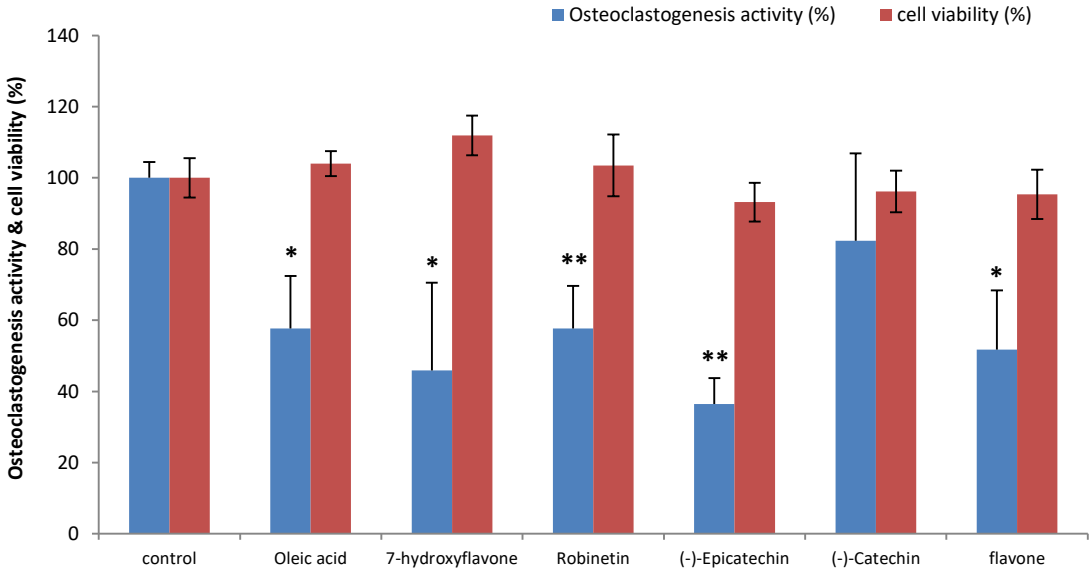

Figure 3.4 *Osteoclastogenesis activity and cell viability of commercial compounds: 7-hydroxyflavone, robinetin, (-)-epicatechin, (-)-catechin and flavone (10µM). Assays were measured in triplet experiment. Each value is expressed as the mean ± SD of triplet determinations. *p < 0.05, **p < 0.01 versus the control group. (Control: DMSO; Oleic acid was used as positive control)*

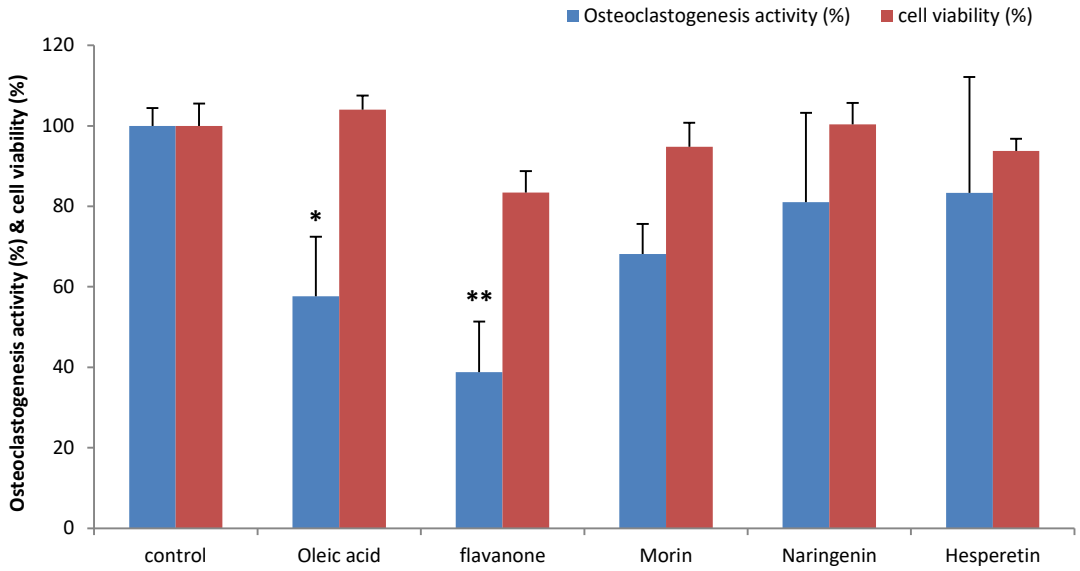

Figure 3.5 *Osteoclastogenesis activity and cell viability of commercial compounds: flavanone, morin, naringenin, and hesperetin (10μM). Assays were measured in triplet experiment. Each value is expressed as the mean ± SD of triplet determinations. *p < 0.05, **p < 0.01 versus the control group. (Control: DMSO; Oleic acid was used as positive control)*

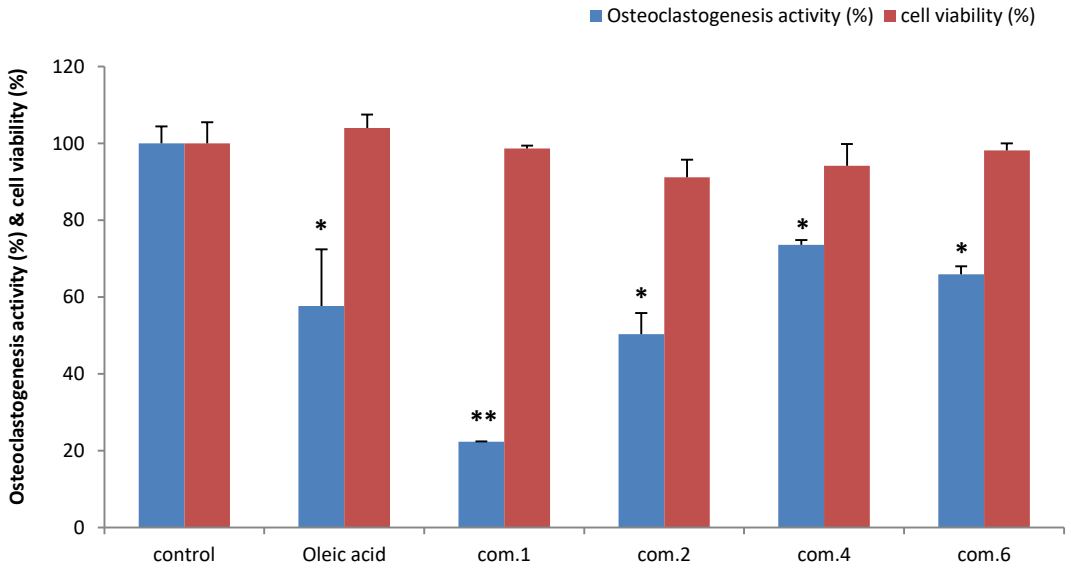

Figure 3.6 *Osteoclastogenesis activity and cell viability of isolated compounds **1**, **2**, **4** and **6** (10μM). Assays were measured in triplet experiment. Each value is expressed as the mean ± SD of triplet determinations. *p < 0.05, **p < 0.01 versus the control group. (Control: DMSO; Oleic acid was used as positive control)*

Table 3 Cell viability and osteoclastogenesis activity of 19 commercial flavonoids

Compound	Cell viability (%)	Osteoclastogenesis activity (%)
Baicalein	100.61±5.94	0.00±0.00**
Luteolin	50.80±5.38*	54.08±30.85
Kaempferol	105.87±3.04*	101.02±11.45
Quercetin	73.00±4.68**	34.69±8.03*
Myricetin	93.48±4.01**	60.20±31.45
Apigenin	88.20±1.86*	51.02±24.51
Galangin	122.13±8.96	27.55±6.61*
Chrysin	133.52±8.19	47.96±26.02
Taxifolin	106.98±6.42	67.06±4.99**
3-hydroxyflavonone	96.60±5.02	41.18±11.65**
7-hydroxyflavonone	111.93±5.58	45.88±24.62*
Robinetin	103.47±8.68	57.65±12.00**
(-)-Epicatechin	93.15±5.42	36.47±7.25**
(-)-Catechin	96.17±5.83	82.35±24.51
Flavone	95.36±6.94	51.76±16.64*
Flavanone	83.45±5.34	38.82±12.56**
Morin	94.83±5.94	68.18±7.42
Naringenin	100.35±5.38	81.06±22.14
Hesperetin	93.76±3.04	83.33±28.83
Oleic acid	103.99±3.53	57.65±14.79*

*Assays were measured in triplet experiment. Each value is expressed as the mean ± SD of triplet determinations. *p < 0.05, **p < 0.01 versus the control group. (Control: DMSO; Oleic acid was used as positive control)*

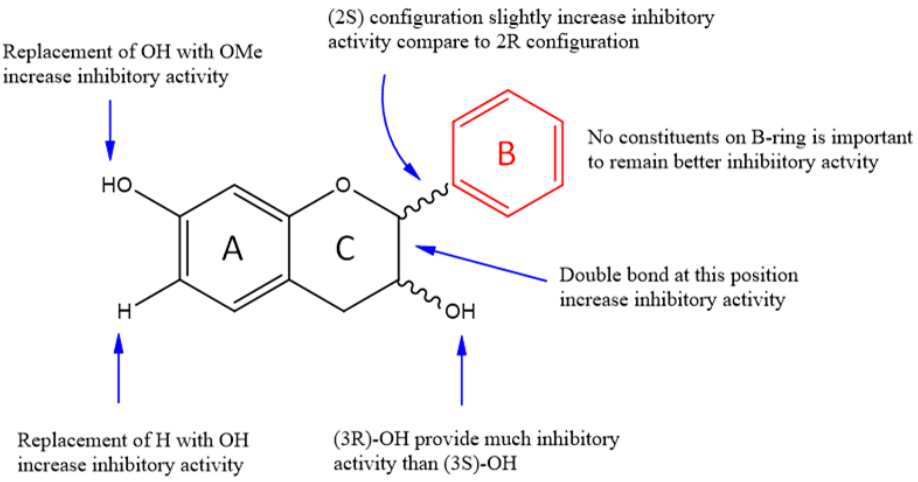

Figure 3.7 Summary of structure-activity relationship of flavonoid skeleton for anti-osteoclastogenesis activity

3.4 Conclusion

Nineteen commercial flavonoids were also performed on anti-osteoclastogenesis activity to establish the early SAR profile in flavonoid skeleton. Among all commercial and isolated compounds, balcalein showed the most effective activity with 100% inhibition on osteoclastogenesis at 10μM; then come to com.1, which is identified as a novel natural flavan and displayed an excellent inhibition on osteoclastogensis with 78% inhibition at 10μM. The absence of substituent in B-ring plays a crucial role in increasing anti-osteoclastogenesis. Interstingly, (3R) configuration of 3-OH provide more effective inhibition than (3S) configuration.

Reference

Albright F, Reifenstein E C. The Parathyriod Glands and Metabolic Bone Disease [J]. The Parathyriod Glands and Metabolic Bone Disease, 1948.

Bao Y, Gao Y, Du M, et al. Topical treatment with Xiaozheng Zhitong Paste (XZP) alleviates bone destruction and bone cancer pain in a rat model of prostate cancer-induced bone pain by modulating the RANKL/RANK/OPG signaling [J]. Evidence-Based Complementary and Alternative Medicine, 2015.

Barros N M T, Hoac B, Neves R L, et al. Proteolytic processing of osteopontin by PHEX and accumulation of osteopontin fragments in Hyp mouse bone, the murine model of X-linked hypophosphatemia [J]. Journal of Bone and Mineral Research, 2013, 28(3): 688-699.

Basle M F, Mazaud P, Malkani K, et al. Isolation of osteoclasts from pagetic bone tissue morphometry and cytochemistry on isolated cells [J]. Bone, 1988, 9(1): 1-6.

Bhansali A. Metabolic bone disease: Newer perspectives [J]. Indian journal of endocrinology and metabolism, 2012, 16(Suppl 2): S140.

Bischi G I, Chiarella C, Kopel M, et al. Overview and Directions for Future Research[M]//Nonlinear Oligopolies. Springer, Berlin, Heidelberg, 2010: 271-274.

Boukpessi T, Gaucher C, Léger T, et al. Abnormal presence of the matrix extracellular phosphoglycoprotein-derived acidic serine-and aspartate-rich motif

peptide in human hypophosphatemic dentin[J]. The American journal of pathology, 2010, 177(2): 803-812.

Boukpessi T, Hoac B, Coyac B R, et al. Osteopontin and the dento-osseous pathobiology of X-linked hypophosphatemia [J]. Bone, 2017, 95: 151-161.

Boyce A M, Florenzano P, de Castro L F, et al. Fibrous dysplasia/McCune-Albrightsyndrome[M]//GeneReviews®[Internet]. University of Washington, Seattle, 2018.

Boyce A M, Kelly M H, Brillante B A, et al. A randomized, double blind, placebo-controlled trial of alendronate treatment for fibrous dysplasia of bone[J]. The Journal of Clinical Endocrinology & Metabolism, 2014, 99(11): 4133-4140.

Cabral C E L, Guedes P, Fonseca T, et al. Polyostotic fibrous dysplasia associated with intramuscular myxomas: Mazabraud's syndrome [J]. Skeletal radiology, 1998, 27(5): 278-282.

Cardillo G, Merlini L, Nasini G, et al. Constituents of Dragon's blood. Part I. Structure and absolute configuration of new optically active flavans [J]. Journal of the Chemical Society C: Organic, 1971: 3967-3970.

Carlin B I, Andriole G L. The natural history, skeletal complications, and management of bone metastases in patients with prostate carcinoma[J]. Cancer:

Interdisciplinary International Journal of the American Cancer Society, 2000, 88(S12): 2989-2994.

Cathomas R, Bajory Z, Bouzid M, et al. Management of bone metastases in patients with castration-resistant prostate cancer[J]. Urologia internationalis, 2014, 92(4): 377-386.

Collin-Osdoby P, Yu X, Zheng H, et al. RANKL-mediated osteoclast formation from murine RAW 264.7 cells[M]//Bone research protocols. Humana Press, 2003: 153-166.

Conte P F, Guarneri V. Safety of intravenous and oral bisphosphonates and compliance with dosing regimens[J]. The Oncologist, 2004, 9(Supplement 4): 28-37.

Corral D A, Amling M, Priemel M, et al. Dissociation between bone resorption and bone formation in osteopenic transgenic mice[J]. Proceedings of the National Academy of Sciences, 1998, 95(23): 13835-13840.

Darnay B G, Haridas V, Ni J, et al. Characterization of the intracellular domain of receptor activator of NF-κB (RANK) Interaction with tumor necrosis factor receptor-associated factors and activation of NF-κB and c-Jun N-terminal kinase[J]. Journal of Biological Chemistry, 1998, 273(32): 20551-20555.

Davidson-Hunt I. Ecological ethnobotany: stumbling toward new practices and paradigms. *MASA J*, 16, 2000, 1-13.

Dearnaley D P, Sydes M R, Mason M D, et al. A double-blind, placebo-controlled, randomized trial of oral sodium clodronate for metastatic prostate cancer (MRC PR05 Trial)[J]. Journal of the National Cancer Institute, 2003, 95(17): 1300-1311.

DiCaprio M R, Enneking W F. Fibrous dysplasia: pathophysiology, evaluation, and treatment[J]. JBJS, 2005, 87(8): 1848-1864.

Gonzales G F, Valerio L G. Medicinal plants from Peru: a review of plants as potential agents against cancer[J]. Anti-Cancer Agents in Medicinal Chemistry (Formerly Current Medicinal Chemistry-Anti-Cancer Agents), 2006, 6(5): 429-444.

Gralow J R, Biermann J S, Farooki A, et al. NCCN task force report: bone health in cancer care[J]. Journal of the National Comprehensive Cancer Network, 2009, 7(Suppl_3): S-1-S-32.

e Lopes M I L, Saffi J, Echeverrigaray S, et al. Mutagenic and antioxidant activities of Croton lechleri sap in biological systems[J]. Journal of Ethnopharmacology, 2004, 95(2-3): 437-445.

Gupta D, Bleakley B, Gupta R K. Dragon's blood: botany, chemistry and therapeutic uses[J]. Journal of ethnopharmacology, 2008, 115(3): 361-380.

Harley R D. Artists' pigments, c. 1600-1835; a study in English documentary sources[J]. 1982.

Hsieh T P, Sheu S Y, Sun J S, et al. Icariin isolated from Epimedium pubescens regulates osteoblasts anabolism through BMP-2, SMAD4, and Cbfa1 expression[J]. Phytomedicine, 2010, 17(6): 414-423.

Hsu H, Lacey D L, Dunstan C R, et al. Tumor necrosis factor receptor family member RANK mediates osteoclast differentiation and activation induced by osteoprotegerin ligand[J]. Proceedings of the National Academy of Sciences, 1999, 96(7): 3540-3545.

Ishida N, Hayashi K, Hoshijima M, et al. Large Scale Gene Expression Analysis of Osteoclastogenesisin Vitro and Elucidation of NFAT2 as a Key Regulator[J]. Journal of Biological Chemistry, 2002, 277(43): 41147-41156.

Jain N, Weinstein R S. Giant osteoclasts after long-term bisphosphonate therapy: diagnostic challenges[J]. Nature Reviews Rheumatology, 2009, 5(6): 341.

Karsenty G, Wagner E F. Reaching a genetic and molecular understanding of skeletal development[J]. Developmental cell, 2002, 2(4): 389-406.

Kawai M, Rosen C J. The insulin-like growth factor system in bone: basic and clinical implications[J]. Endocrinology and Metabolism Clinics, 2012, 41(2): 323-333.

Keller J, Brink S, Busse B, et al. Divergent resorbability and effects on osteoclast formation of commonly used bone substitutes in a human in vitro-assay[J]. PloS one, 2012, 7(10): e46757.

Kong Y Y, Yoshida H, Sarosi I, et al. OPGL is a key regulator of osteoclastogenesis, lymphocyte development and lymph-node organogenesis[J]. Nature, 1999, 397(6717): 315.

Kozyrakis D, Paridis D, Perikleous S, et al. The Current Role of Osteoclast Inhibitors in Patients with Prostate Cancer[J]. Advances in urology, 2018, 2018

Lee J S, FitzGibbon E J, Chen Y R, et al. Clinical guidelines for the management of craniofacial fibrous dysplasia[C]//Orphanet journal of rare diseases. BioMed Central, 2012, 7(1): S2.

Lei S F, Chen Y, Xiong D H, et al. Ethnic difference in osteoporosis-related phenotypes and its potential underlying genetic determination[J]. Journal of Musculoskeletal and Neuronal Interactions, 2006, 6(1): 36.

Liu J, Shiono J, Tsuji Y, et al. Methyl ganoderic acid DM: a selective potent osteoclastogenesis inhibitor[J]. The Open Bioactive Compounds Journal, 2009, 2(1).

Lu S H, Chen T H, Chou T C. Magnolol Inhibits RANKL-induced osteoclast differentiation of raw 264.7 macrophages through heme oxygenase-1-dependent inhibition of NFATc1 expression[J]. Journal of natural products, 2015, 78(1): 61-68.

Manolagas S C. Birth and death of bone cells: basic regulatory mechanisms and implications for the pathogenesis and treatment of osteoporosis[J]. Endocrine reviews, 2000, 21(2): 115-137.

McInnes I B, Schett G. The pathogenesis of rheumatoid arthritis[J]. New England Journal of Medicine, 2011, 365(23): 2205-2219.

McKee M D, Hoac B, Addison W N, et al. Extracellular matrix mineralization in periodontal tissues: Noncollagenous matrix proteins, enzymes, and relationship to hypophosphatasia and X-linked hypophosphatemia[J]. Periodontology 2000, 2013, 63(1): 102-122.

Mohamed S G K, Sugiyama E, Shinoda K, et al. Interleukin-10 inhibits RANKL-mediated expression of NFATc1 in part via suppression of c-Fos and c-Jun in RAW264. 7 cells and mouse bone marrow cells[J]. Bone, 2007, 41(4): 592-602.

Miyamoto I, Liu J, Shimizu K, et al. Regulation of osteoclastogenesis by ganoderic acid DM isolated from Ganoderma lucidum[J]. European journal of pharmacology, 2009, 602(1): 1-7.

Muralidharan A, Smith M T. Pathobiology and management of prostate cancer-induced bone pain: recent insights and future treatments[J]. Inflammopharmacology, 2013, 21(5): 339-363.

Notelovitz M. Osteoporosis: screening, prevention, and management[J]. Fertility and sterility, 1993, 59(4): 707-725.

Palmieri C, Fullarton J R, Brown J. Comparative efficacy of bisphosphonates in metastatic breast and prostate cancer and multiple myeloma: a mixed-treatment meta-analysis[J]. Clinical Cancer Research, 2013, 19(24): 6863-6872.

Paul Tuck S, Layfield R, Walker J, et al. Adult Paget's disease of bone: a review [J]. Rheumatology, 2017, 56(12): 2050-2059.

Plotkin H, Rauch F, Zeitlin L, et al. Effect of pamidronate treatment in children with polyostotic fibrous dysplasia of bone[J]. The Journal of Clinical Endocrinology & Metabolism, 2003, 88(10): 4569-4575.

Raisz L G, Rodan G A. Pathogenesis of osteoporosis[J]. Endocrinology and metabolism clinics of North America, 2003, 32(1): 15-24.

Ralston S H, Layfield R. Pathogenesis of Paget disease of bone [J]. Calcified tissue international, 2012, 91(2): 97-113.

Rodan G A, Fleisch H A. Bisphosphonates: mechanisms of action[J]. The Journal of clinical investigation, 1996, 97(12): 2692-2696.

Rogers M J, Gordon S, Benford H L, et al. Cellular and molecular mechanisms of action of bisphosphonates[J]. Cancer: Interdisciplinary International Journal of the American Cancer Society, 2000, 88(S12): 2961-2978.

Rosen L S, Gordon D, Kaminski M, et al. Zoledronic acid versus pamidronate in the treatment of skeletal metastases in patients with breast cancer or osteolytic lesions of

multiple myeloma: a phase III, double-blind, comparative trial[J]. Cancer journal (Sudbury, Mass.), 2001, 7(5): 377-387.

Ross F P. M-CSF, c-Fms, and signaling in osteoclasts and their precursors[J]. Annals of the New York Academy of Sciences, 2006, 1068(1): 110-116.

Rossi D, Bruni R, Bianchi N, et al. Evaluation of the mutagenic, antimutagenic and antiproliferative potential of Croton lechleri (Muell. Arg.) latex[J]. Phytomedicine, 2003, 10(2-3): 139-144.

Saraswathy A, Vidhya B. (+)-Afzelechin from the rhizome of Calamus rotang Linn[J]. Indian drugs, 2012, 49(49): 49-50.

Sato K, Takayanagi H. Osteoclasts, rheumatoid arthritis, and osteoimmunology[J]. Current opinion in rheumatology, 2006, 18(4): 419-426.

Simonet W S, Lacey D L, Dunstan C R, et al. Osteoprotegerin: a novel secreted protein involved in the regulation of bone density[J]. cell, 1997, 89(2): 309-319.

Smith M R, Saad F, Coleman R, et al. Denosumab and bone-metastasis-free survival in men with castration-resistant prostate cancer: results of a phase 3, randomised, placebo-controlled trial[J]. The Lancet, 2012, 379(9810): 39-46.

Sukari S, Said I M. Phenolic Compounds from the Fruits of Orania Sylvicola[J]. Malaysian Journal of Analytical Sciences, 2013, 17(2): 276-280.

Syafni N, Putra D P, Arbain D. 3, 4-dihydroxybenzoic acid and 3, 4-dihydroxybenzaldehyde from the fern Trichomanes chinense L.; isolation, antimicrobial and antioxidant properties[J]. Indonesian Journal of Chemistry, 2012, 12(3): 273-278.

Takayanagi H. The role of NFAT in osteoclast formation[J]. Annals of the New York Academy of Sciences, 2007, 1116(1): 227-237.

Tan H, Furuta S, Nagata T, et al. Inhibitory effects of the leaves of loquat (Eriobotrya japonica) on bone mineral density loss in ovariectomized mice and osteoclast differentiation [J]. Journal of agricultural and food chemistry, 2014, 62(4): 836-841.

Teitelbaum S L, Ross F P. Genetic regulation of osteoclast development and function[J]. Nature Reviews Genetics, 2003, 4(8): 638.

Vincent C, Kogawa M, Findlay D M, et al. The generation of osteoclasts from RAW 264.7 precursors in defined, serum-free conditions[J]. Journal of bone and mineral metabolism, 2009, 27(1): 114-119.

Wada T, Nakashima T, Hiroshi N, et al. RANKL–RANK signaling in osteoclastogenesis and bone disease[J]. Trends in molecular medicine, 2006, 12(1): 17-25.

Wagner E F, Karsenty G. Genetic control of skeletal development[J]. Current opinion in genetics & development, 2001, 11(5): 527-532.

Wu Y B, Zheng C J, Qin L P, et al. Antiosteoporotic activity of anthraquinones from Morinda officinalis on osteoblasts and osteoclasts[J]. Molecules, 2009, 14(1): 573-583.

Yamashita T, Yao Z, Li F, et al. NF-kB p50 and p52 regulate RANKL and TNF-induced osteoclast precursor differentiation by activating c-Fos and NFATc1[J]. Journal of Biological Chemistry, 2007.

Yasuda H, Shima N, Nakagawa N, et al. Osteoclast differentiation factor is a ligand for osteoprotegerin/osteoclastogenesis-inhibitory factor and is identical to TRANCE/RANKL[J]. Proceedings of the National Academy of Sciences, 1998, 95(7): 3597-3602.

Yokoyama S, Bang T H, Shimizu K, et al. Osteoclastogenesis inhibitory effect of ergosterol peroxide isolated from Pleurotus eryngii[J]. Natural product communications, 2012, 7(9): 1934578X1200700913.

Zhang G, Qin L, Hung W Y, et al. Flavonoids derived from herbal Epimedium Brevicornum Maxim prevent OVX-induced osteoporosis in rats independent of its enhancement in intestinal calcium absorption[J]. Bone, 2006, 38(6): 818-825.

Zhang D, Zhang J, Fong C, et al. Herba epimedii flavonoids suppress osteoclastic differentiation and bone resorption by inducing G2/M arrest and apoptosis[J]. Biochimie, 2012, 94(12): 2514-2522.

ZHAO X, FENG Y, Yong P. Prevention and treatment of osteoporosis with Chinese herbal medicines[J]. Chinese Herbal Medicines, 2012, 4(4): 265-270.

https://en.wikipedia.org/wiki/Paget%27s_disease_of_bone#cite_note-22

https://www.niams.nih.gov/health-topics/osteoporosis

https://rarediseases.info.nih.gov/diseases/5700/rickets

https://rarediseases.org/rare-diseases/rickets-vitamin-d-deficiency/

Appendix

NMR spectrum of two novel isolated compounds

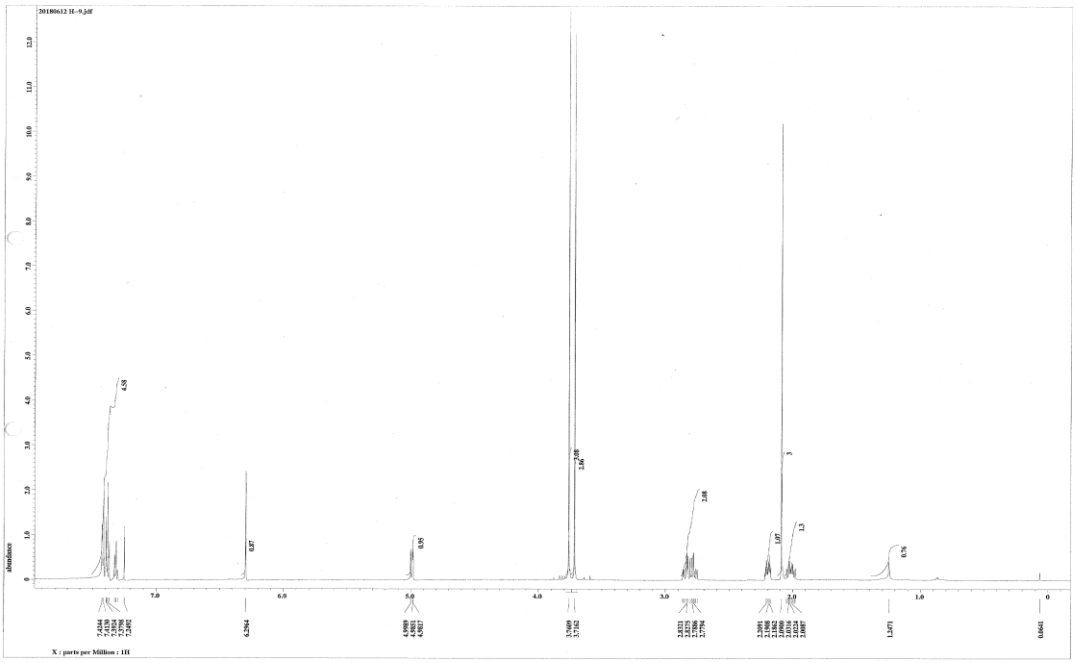

Figure S2.1 ^{1}H NMR spectrum ($CDCl_3$) of (2S)-5,7-dimethoxy-6-methylflavan (**1**)

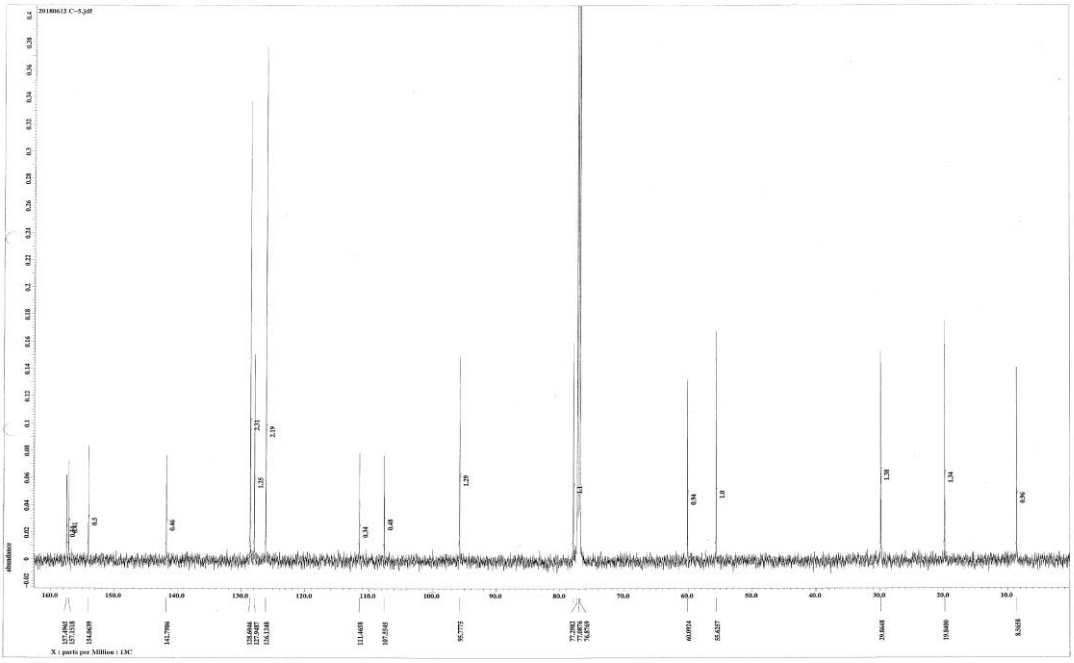

Figure S2.2 ^{13}C NMR spectrum ($CDCl_3$) of (2S)-5,7-dimethoxy-6-methylflavan (**1**)

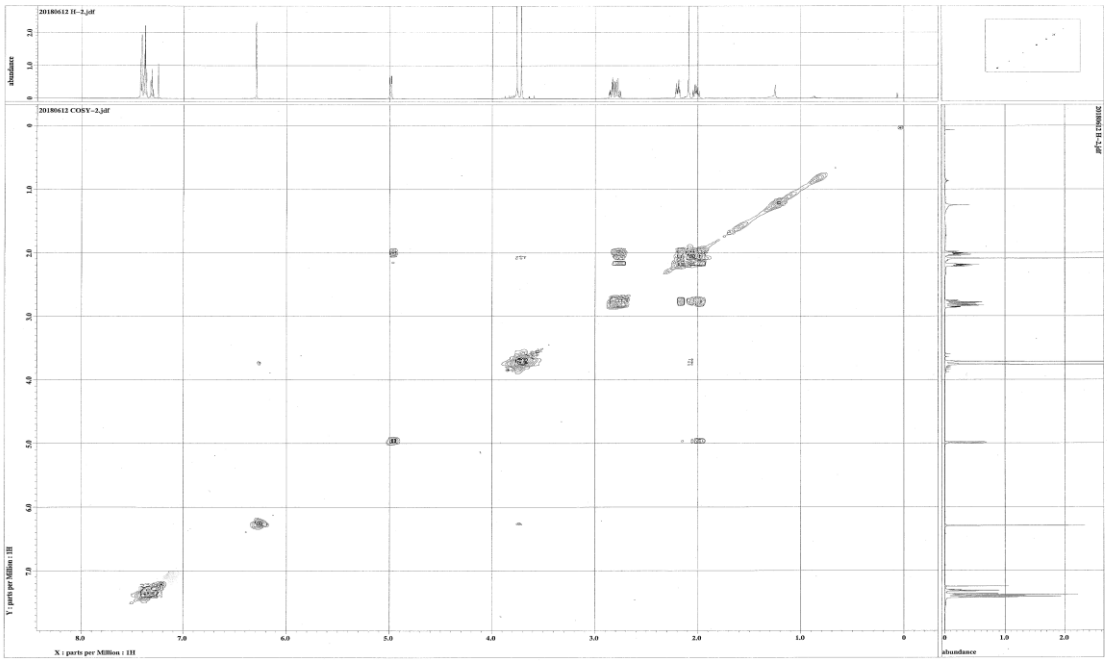

Figure S2.3 ^{1}H-^{1}H COSY spectrum ($CDCl_3$) of (2S)-5,7-dimethoxy-6-methylflavan (**1**)

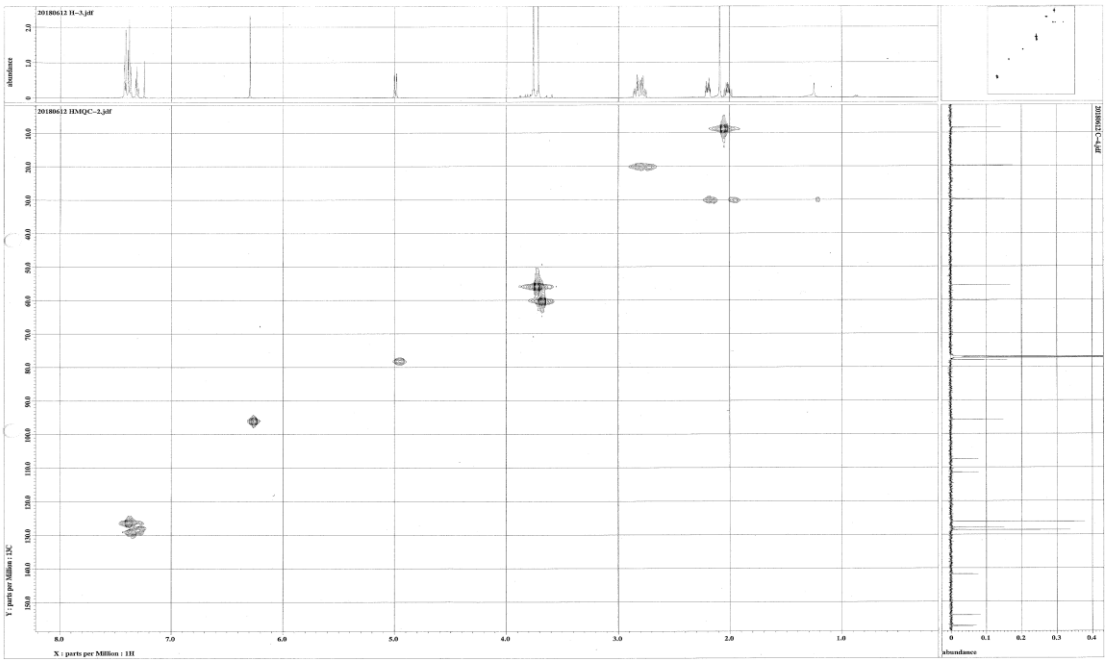

Figure S2.5 HMQC spectrum ($CDCl_3$) of (2S)-5,7-dimethoxy-6-methylflavan (**1**)

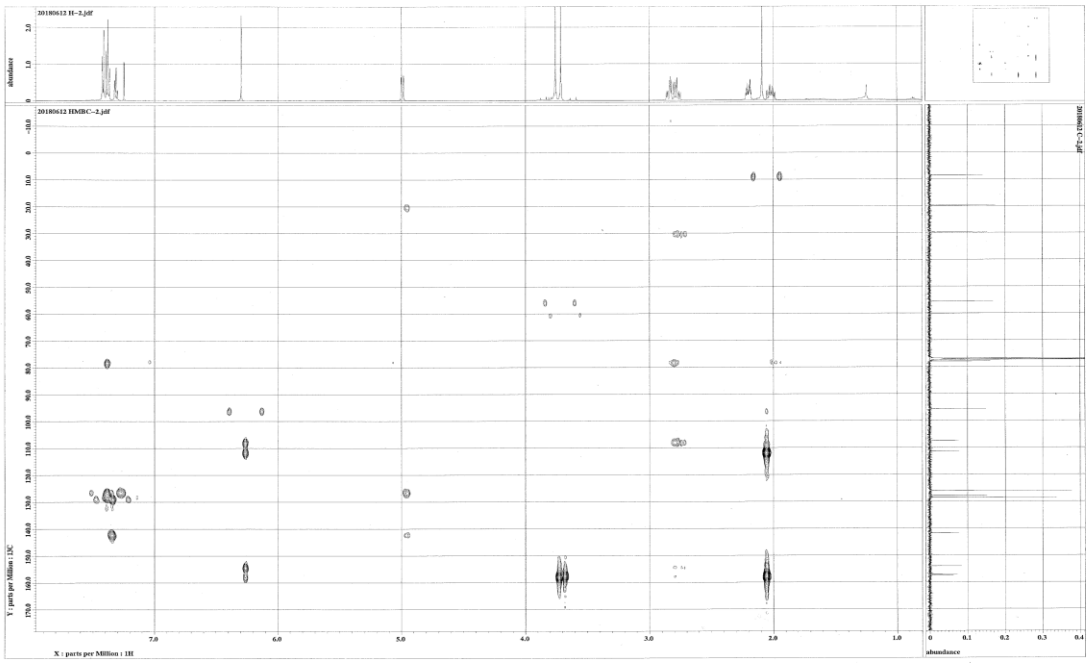

Figure S2.6 HMBC spectrum ($CDCl_3$) of (2S)-5,7-dimethoxy-6-methylflavan (**1**)

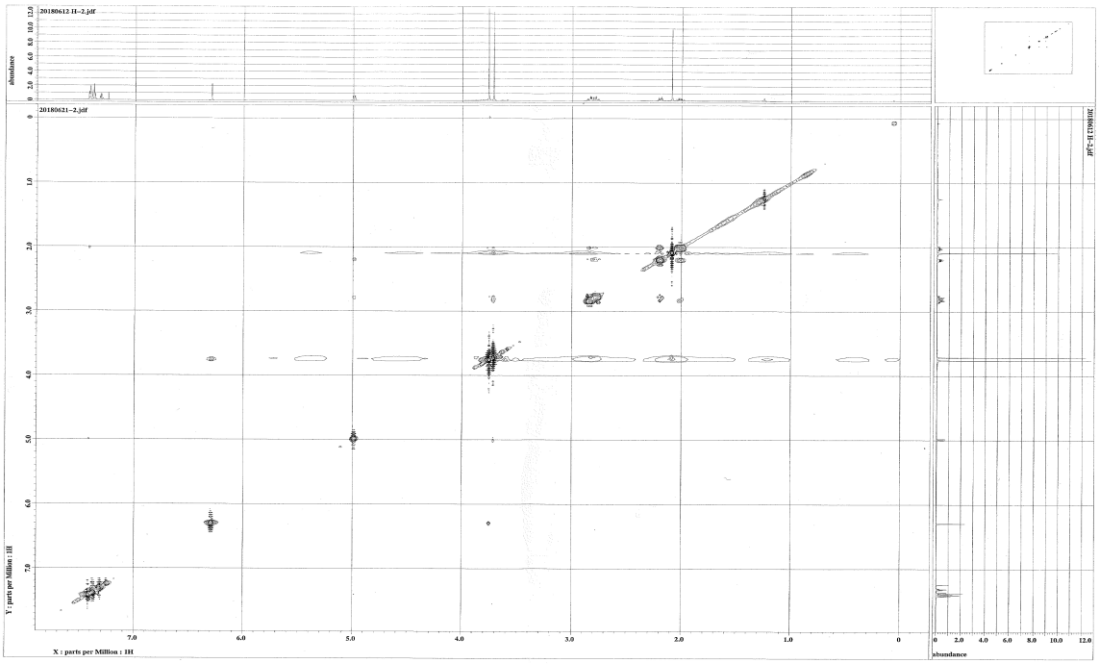

Figure S2.6 NOESY spectrum ($CDCl_3$) of (2S)-5,7-dimethoxy-6-methylflavan (**1**)

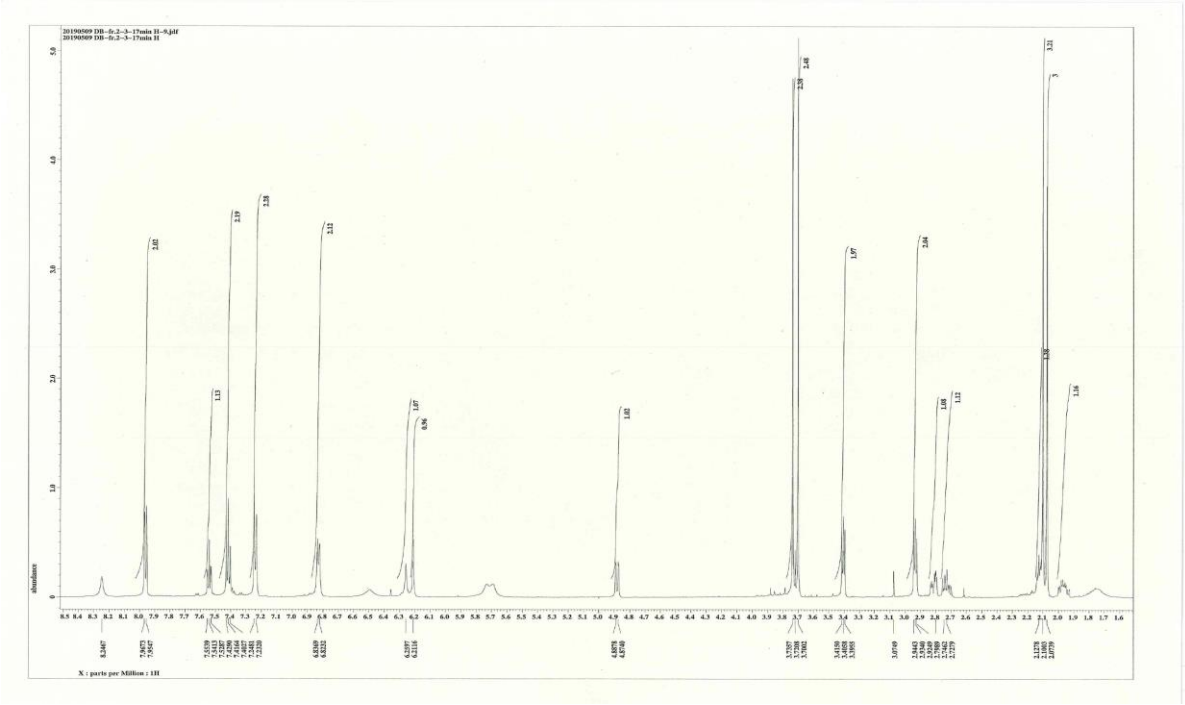

Figure S2.7 ^{1}H NMR spectrum ($CDCl_3$) of (2R)-3-(4-hydroxy-6-((2-(4-hydroxyphenyl)-5-methoxy-6-methylchroman-7-yl)oxy)-2-methoxy-3-methylphenyl)-1-phenylpropan-1-one (**2**)

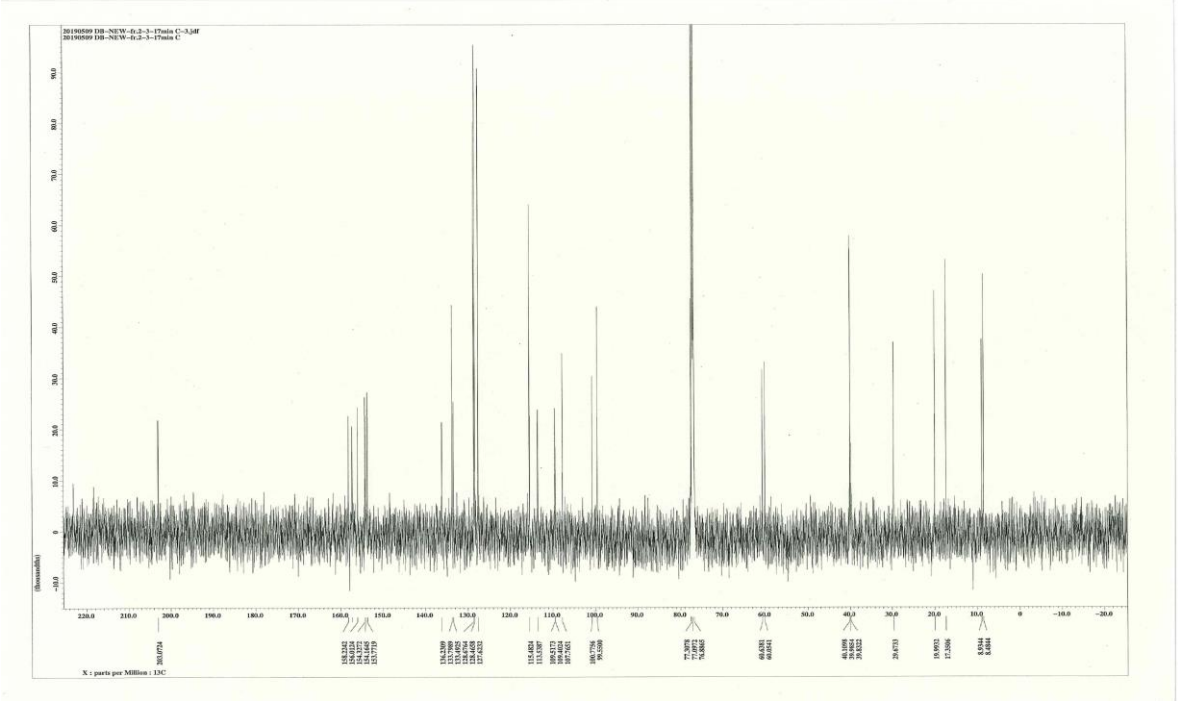

Figure S2.8 ^{13}C NMR spectrum ($CDCl_3$) of (2R)-3-(4-hydroxy-6-((2-(4-hydroxyphenyl)-5-methoxy-6-methylchroman-7-yl)oxy)-2-methoxy-3-methylphenyl)-1-phenylpropan-1-one (**2**)

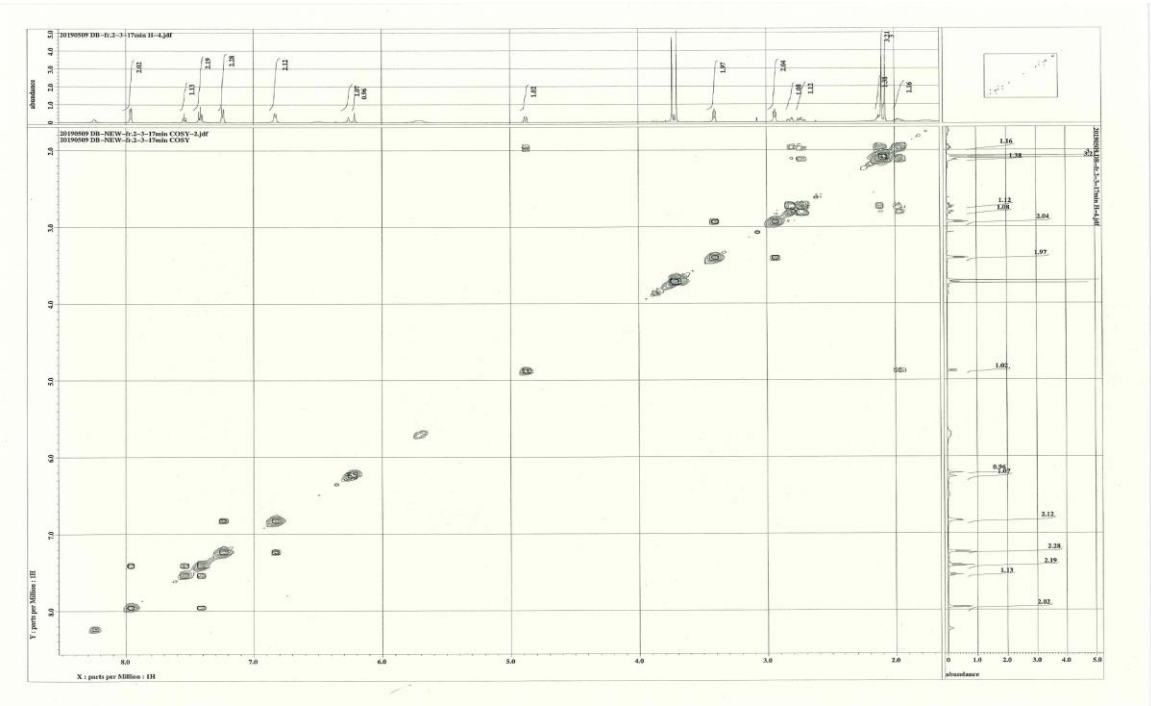

Figure S2.9 ^{1}H-^{1}H COSY spectrum ($CDCl_3$) of (2R)-3-(4-hydroxy-6-((2-(4-hydroxyphenyl)-5-methoxy-6-methylchroman-7-yl)oxy)-2-methoxy-3-methylphenyl)-1-phenylpropan-1-one (**2**)

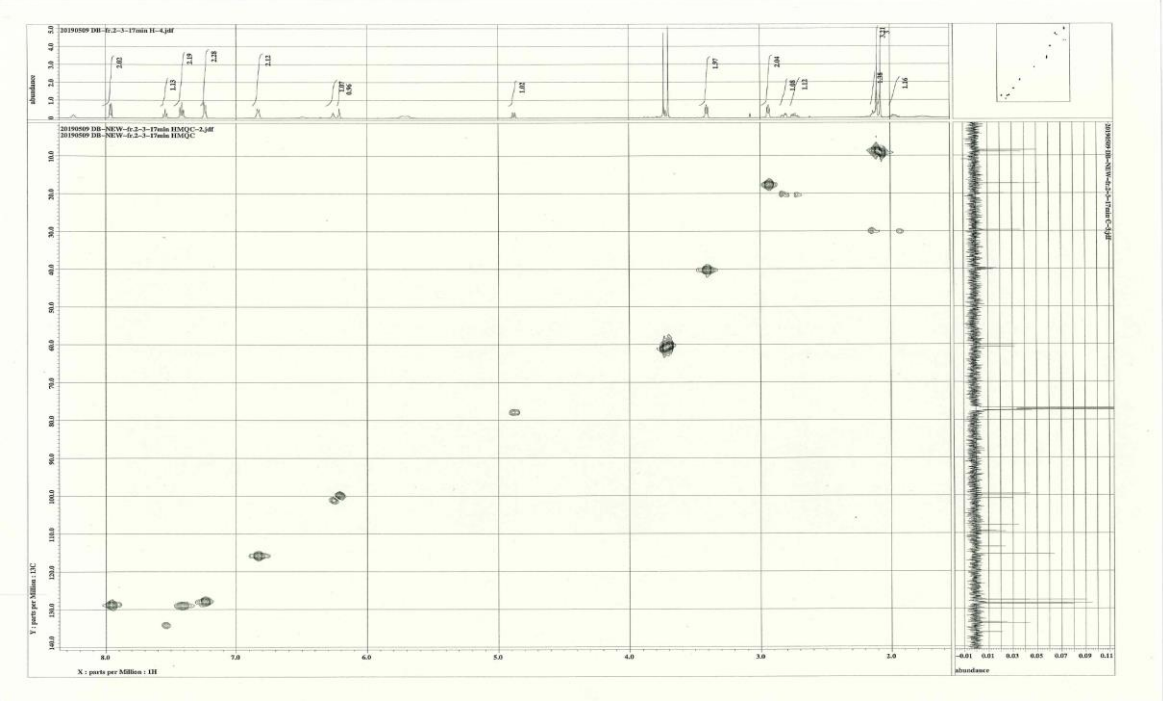

Figure S2.10 HMQC spectrum ($CDCl_3$) of (2R)-3-(4-hydroxy-6-((2-(4-hydroxyphenyl)-5-methoxy-6-methylchroman-7-yl)oxy)-2-methoxy-3-methylphenyl)-1-phenylpropan-1-one (**2**)

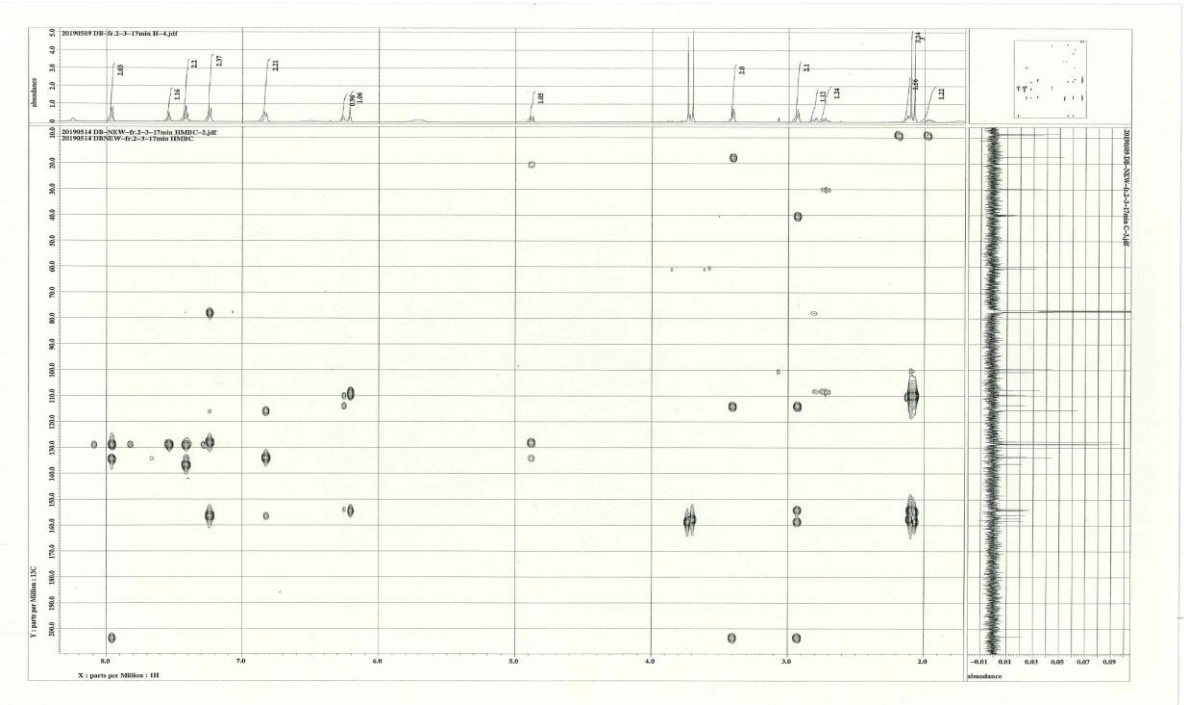

Figure S2.11 HMBC spectrum ($CDCl_3$) of (2R)-3-(4-hydroxy-6-((2-(4-hydroxyphenyl)-5-methoxy-6-methylchroman-7-yl)oxy)-2-methoxy-3-methylphenyl)-1-phenylpropan-1-one (**2**)

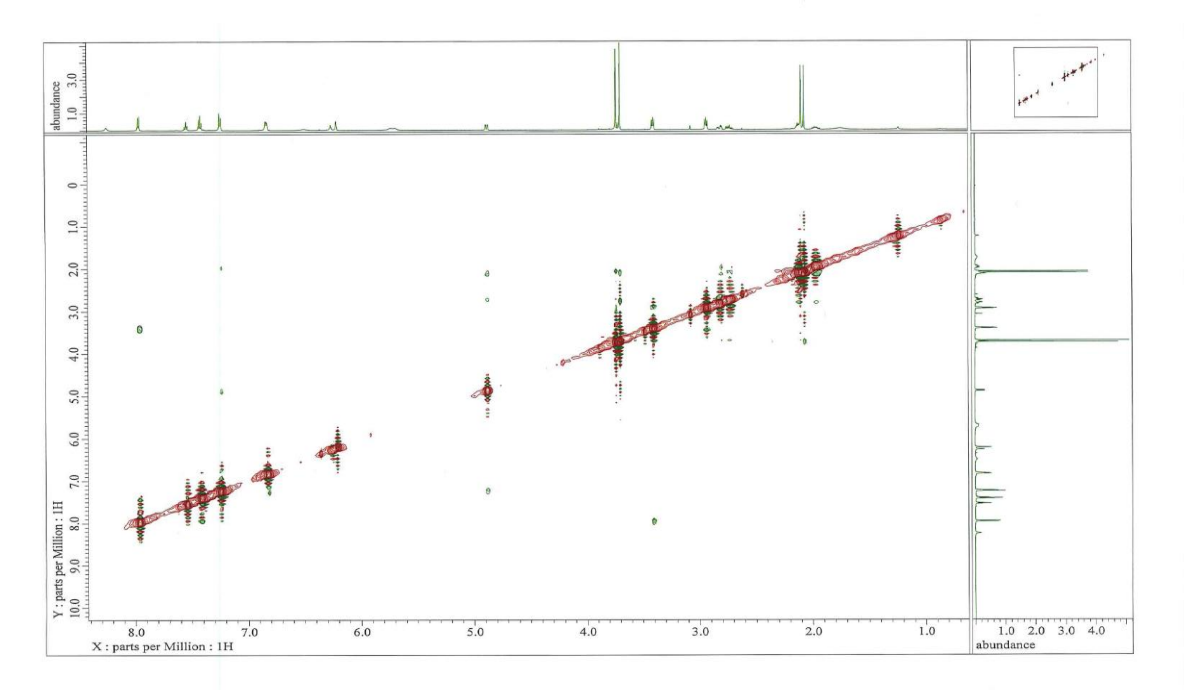

Figure S2.11 NOESY spectrum ($CDCl_3$) of (2R)-3-(4-hydroxy-6-((2-(4-hydroxyphenyl)-5-methoxy-6-methylchroman-7-yl)oxy)-2-methoxy-3-methylphenyl)-1-phenylpropan-1-one (**2**)